

Saving the Fuel Cell Dream: Making Non Noble Metal Electrocatalysts a Reality?

Sanjeev Mukerjee

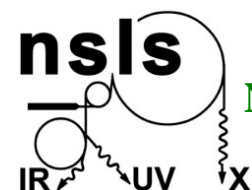
Nagappan Ramaswamy, Urszula Tylus, and Qingying Jia



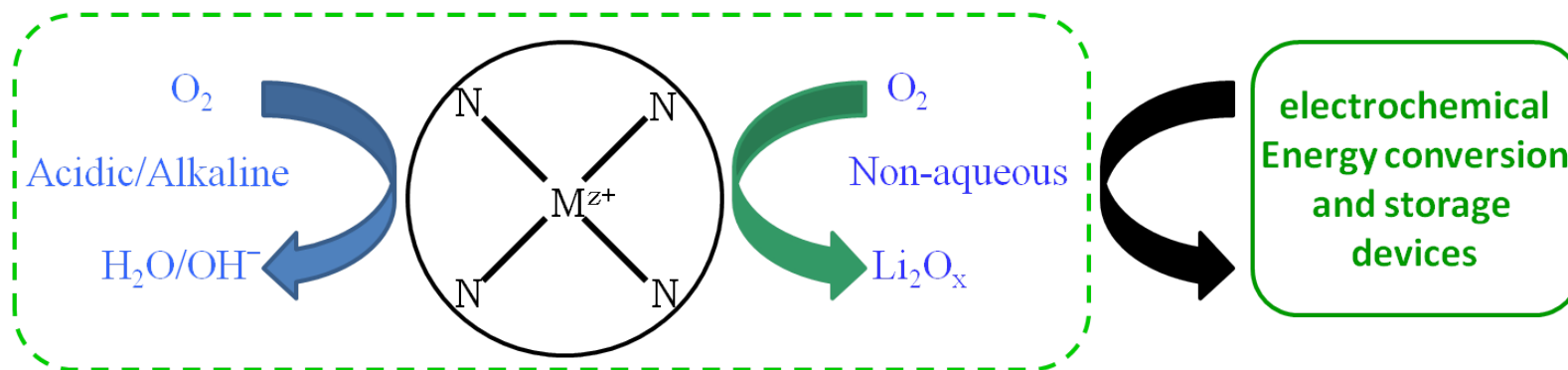
Department of Chemistry & Chemical Biology

Northeastern University Center for Renewable Energy Technology (NUCRET)

Northeastern University, Boston

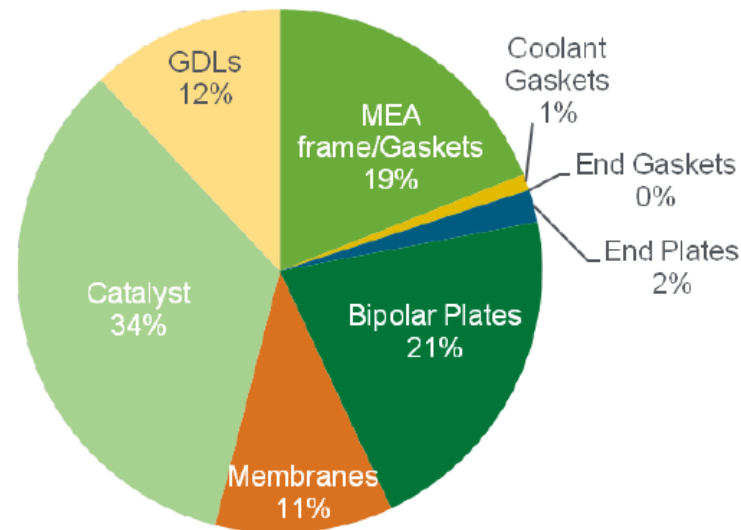


Overarching Electrochemical Oxygen Reduction Reaction \longleftrightarrow Renewable Energy



Need to Replace Pt and Pt Alloys

Polymer Electrolyte Fuel Cell Stack Cost (\$26/kW)



Analysis:

- Scaled to high-volume production of 500,000 units/year
- Assumed Pt cost of \$1100/oz

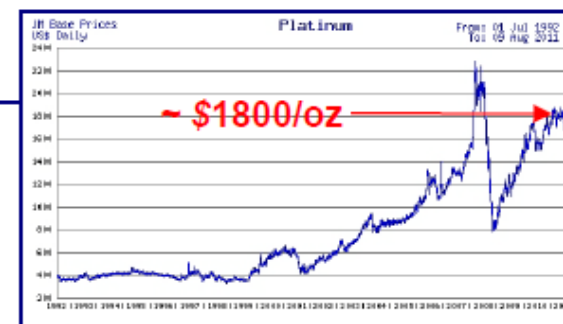
Challenges:

- Platinum cost representing ~34% of total stack cost
- Catalyst durability in need of improvement

James *et al.*, DTI, Inc., 2010 DOE Hydrogen Program Review, Washington, DC, June 9, 2010

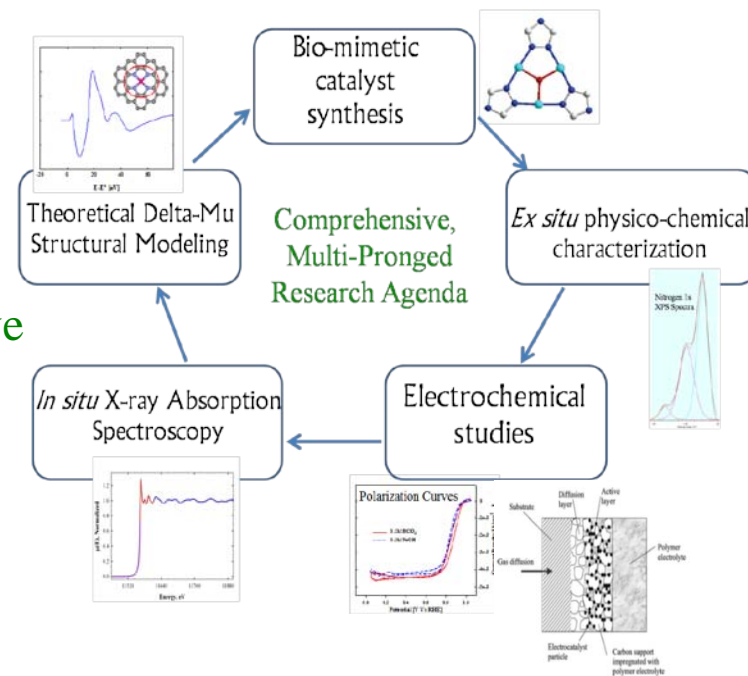
Main strategies to address catalyst cost challenge:

- Reduction in the platinum group metal (PGM) content
- Improvements to Pt catalyst utilization and durability
- Pt alloy catalysts with comparable performance to Pt but costing less
- Non-precious metal catalysts with improved performance and durability



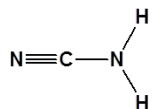
Outline:

- State of the art performance for Non PGM catalysts
- How close are we to Pt ?
- Are these Durable ?
- Literature Review on Metal-free versus $M-N_x$ Active Sites
- Some Mechanistic Principles
- Fundamental understanding using Model Systems
 - Metal-Porphyrin Precursor
 - Cross Laboratory Comparative Study
 - Acid versus Alkaline Perspective
 - Nature of the Active Site
- Knowledge beyond the nature of the active site: Volcano vs. Redox Potentials??

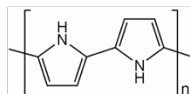


Representative LANL Approach:

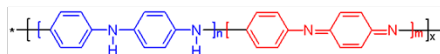
Cyanamide



Polypyrrole



Polyaniline



Carbon support

Transition metal

First heat treatment at up to 1100°C in inert atmosphere

0.5 M H₂SO₄ leach at 80-90°C

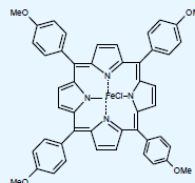
Second heat treatment at 900°C in inert atmosphere

ORR performance evaluation; characterization

Fe precursor

- Fe salt
- Fe complex

like porphyrin



Cl-FeTMPP

N precursor

- NH₃
- CH₃CN
- Fe complex like porphyrin

- N-polymer like PAN, polypyrrole, polyaniline

C support

- Carbon black
- Activated carbon
- Ball-milled graphite
- Carbon nanotubes

Pyrolysis step

- 500-1100°C

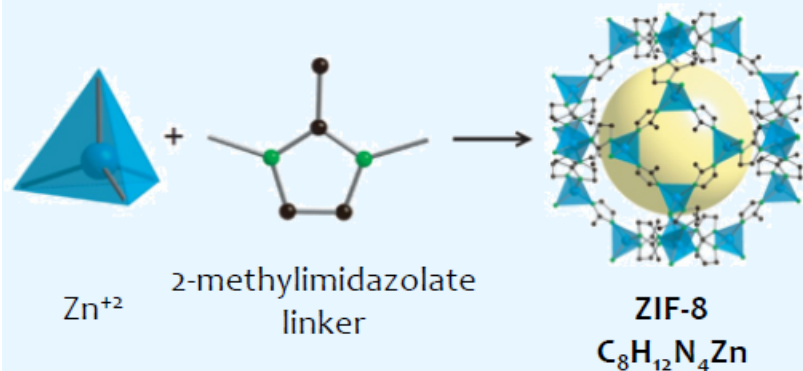
INRS-Dodelet Group: Pior Approach



Our choices:

Method: Wet Impregnation
 Fe precursor: Fe^{II}Ac (ferrous acetate)
 N precursor: NH₃ (ammonia)
 C support: Various carbon supports
 Pyrolysis step: 900 to 1000°C

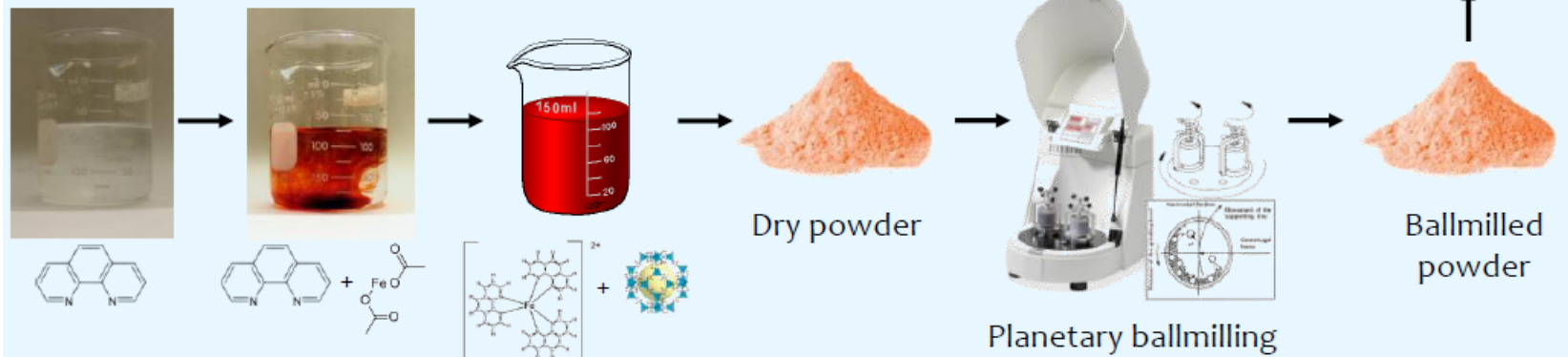
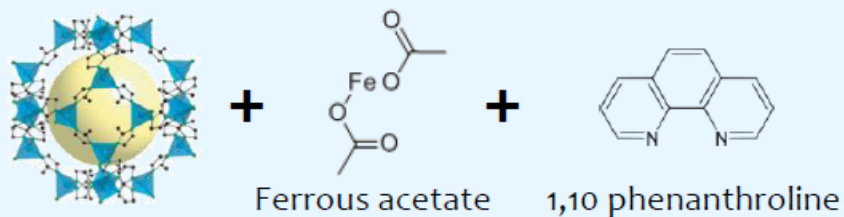
Current INRS-Canetique Approach:



ZIF-8 is a commercial zeolitic imidazolate framework
 Surface area $\sim 2000 \text{ m}^2/\text{g}$
 Pore diameter (yellow sphere) = 1.16 nm
 Thermally stable up to $\sim 500^\circ\text{C}$ in N_2
 Chemically stable in air at room temp.

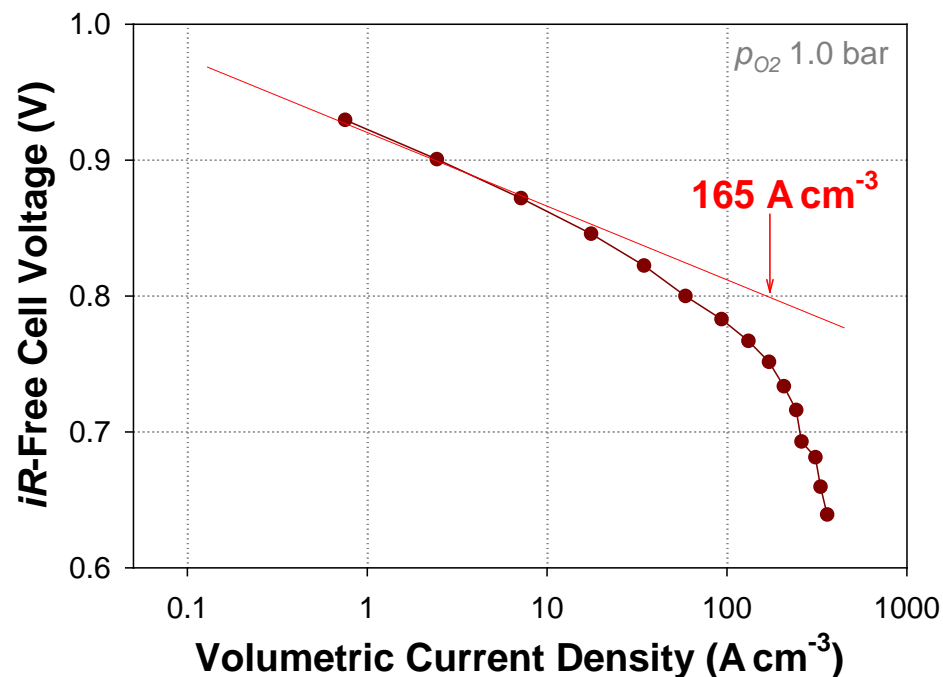
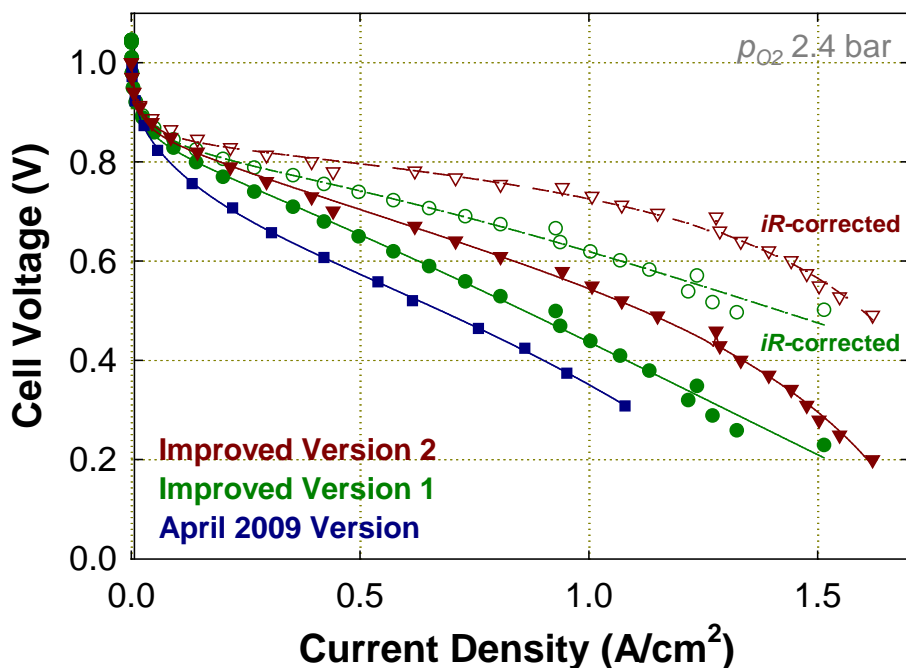
K. S. Park et al. ...O. M. Yaghi, PNAS 103, 10186-10191 (2006)

We replaced the highly microporous carbon support with ZIF-8



Cyanamide-Fe-C Catalyst: Performance-LANL

Anode: $0.25 \text{ mg cm}^{-2} \text{ Pt (E-TEK)}$; Cathode: $\sim 3.5 \text{ mg cm}^{-2} \text{ CM-Fe-C}$; Membrane: Nafion® 117 Cell: 80°C



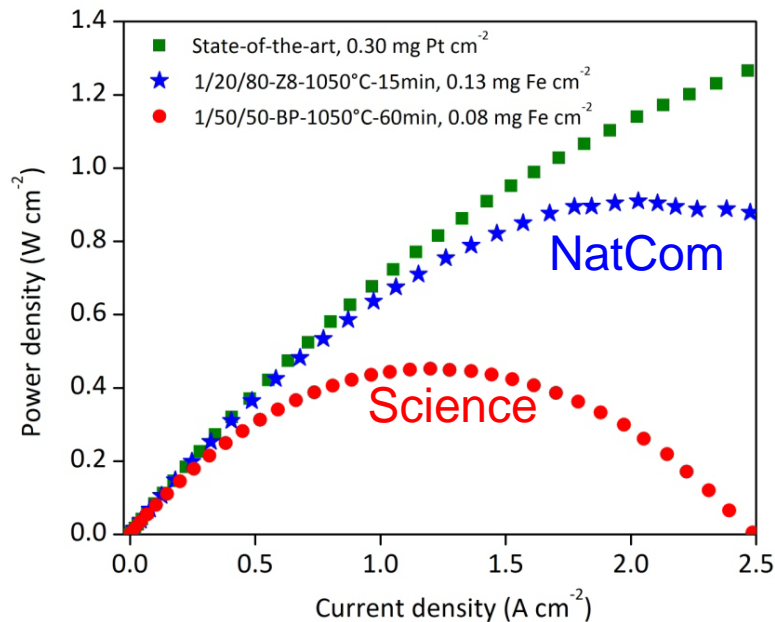
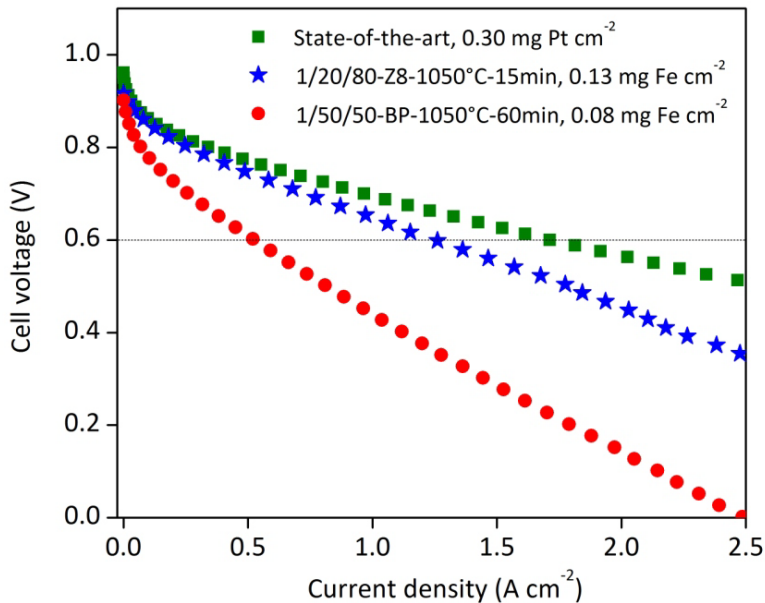
- **Version 1** achieved with change in the carbon support and adjustment of precursor ratios
- **Version 2** generated by including additional sulfur-containing precursor

0.39 A cm^{-2} – measured per MEA surface area at 0.80 V (*iR*-corrected)

60 A cm^{-3} – measured per electrode volume at 0.80 V (*iR*-corrected)

165 A cm^{-3} – extrapolated per electrode volume at 0.80 V (*iR*-corrected)

Best catalyst in 2011 (INRS-NatComm)

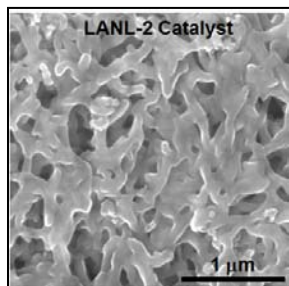


1. Impregnation on Basolite Z1200 (80%wt) with phenanthroline (20%wt) and iron acetate (1%wt Fe)
2. Ball-milling of the precursor
3. First pyrolysis at 1050°C under Ar, 60 min
4. Second pyrolysis at 950°C under NH_3 , to obtain final mass loss of 90%wt after the two pyrolysis

Fuel cell tests at 80°C , H_2/O_2 , fully humidified, Nafion NRE211
 $\approx 4 \text{ mg / cm}^2$ of NatCom Catalyst
or of Science catalyst
Back Pressure: 100 kPa
(200 kPa total with atmospheric pressure)

E. Proietti, F. Jaouen, M. Lefèvre, N. Larouche, J. Tian, J. Herranz, and J.P. Dodelet, *Nature Communications*, **2**, 416 (2011)

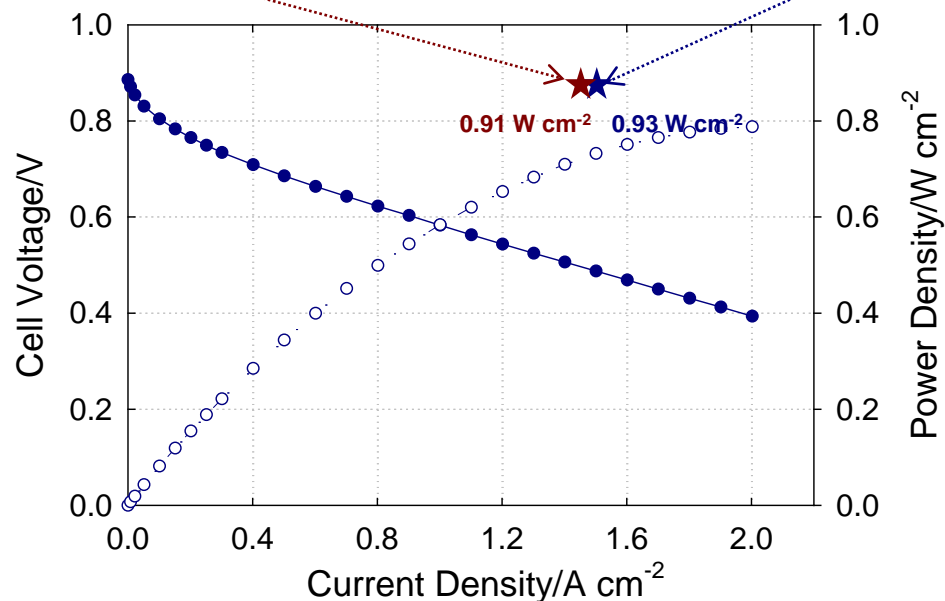
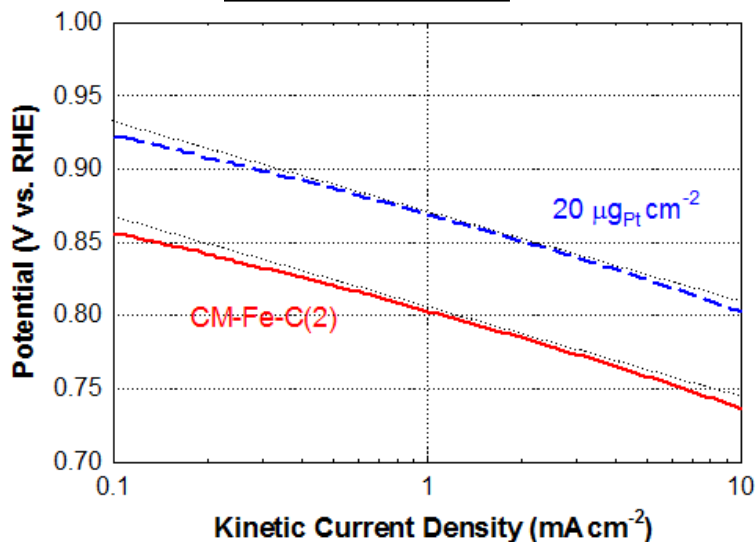
How Far are We From Pt: Not too far I imagine



Anode: 0.5 mg cm^{-2} Pt (E-TEK) 1 bar(applied) H_2 200 sccm; Cathode: $\sim 3.5 \text{ mg cm}^{-2}$ 1 bar(applied) O_2 200 sccm; Membrane: Nafion® 212; Cell: 80°C

Proietti et al., Nat. Commun. 2, 416 (2011):
Membrane: Nafion®211; cathode: 3.9 mg cm^{-2}

“LANL-2” after correction for
membrane thickness difference



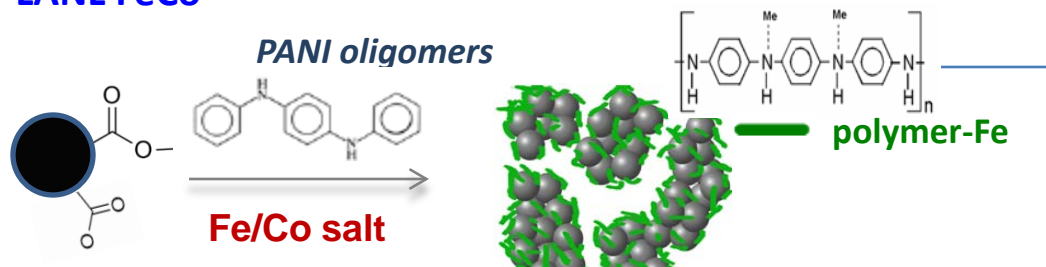
- $\sim 70 \text{ mV}$ difference in $E_{1/2}$ between CM-Fe-C catalyst and Pt reference catalyst ($20 \mu\text{g}_{\text{Pt}} \text{ cm}^{-2}$)
- H_2O_2 generation: $\sim 1\%$
- Tafel slope of CM-Fe-C catalyst in RDE testing: $\sim 61 \text{ mV/dec}$

- High power density of 0.80 W cm^{-2} at 0.40 V recorded
- Power density measured comparable to that published by Proietti et al. (after a membrane-thickness correction)

“LANL2” Catalyst with Improved Oxygen Mass Transport

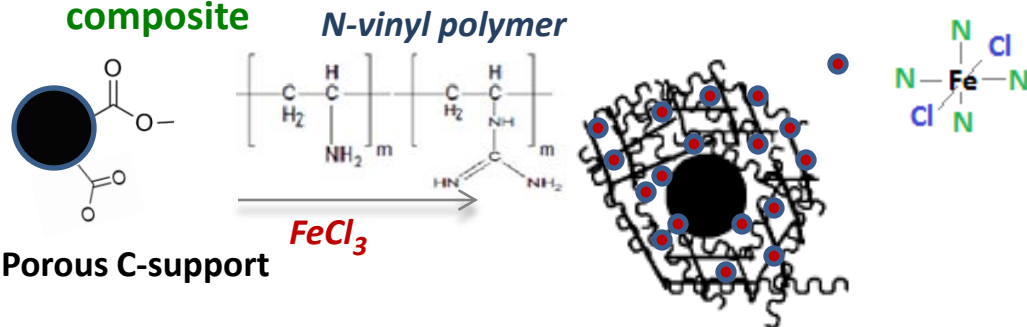
Other MNC Electrocatalysts: Various Synthesis pathways

❖ LANL FeCo



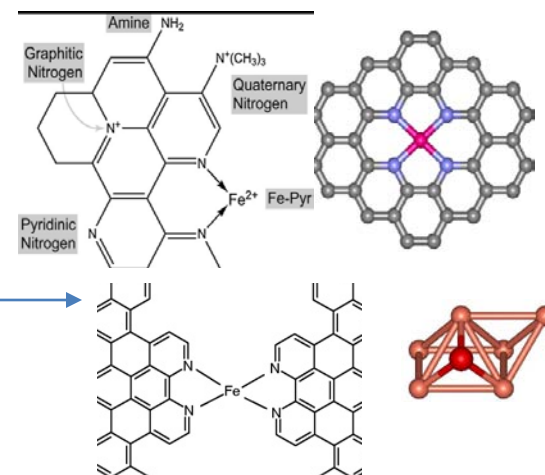
Porous C-support

❖ NEU Fe-Vinyl composite



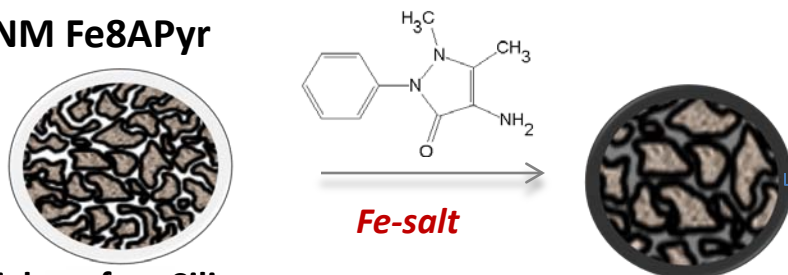
Porous C-support

High temp.
Pyrolysis
700-1000C



M-N-C catalyst

❖ UNM Fe₈APyr

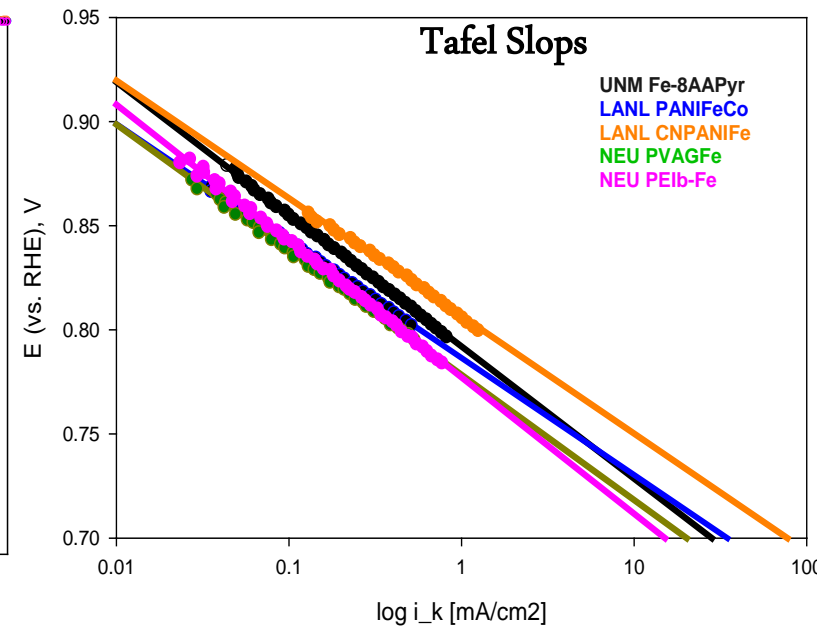
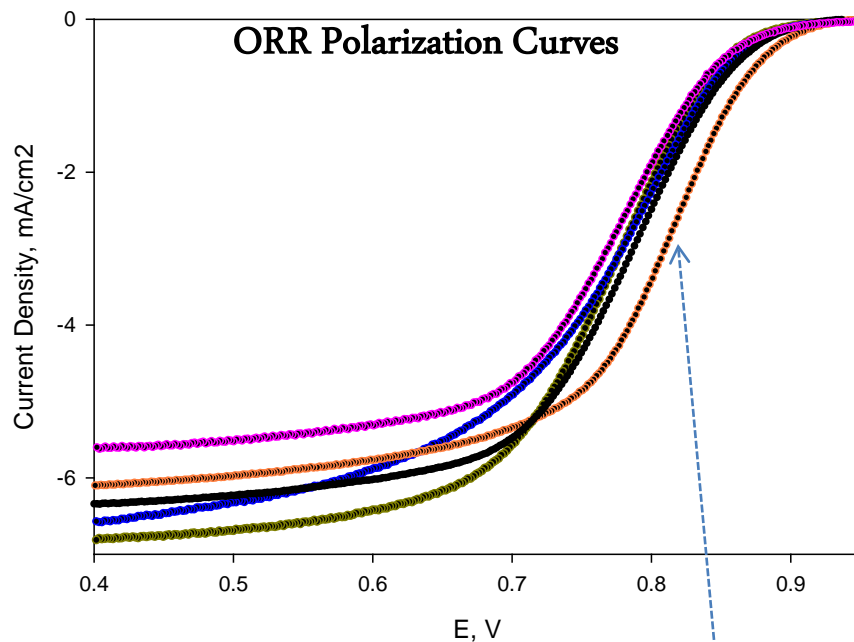


High surface Silica
– template

Comparative ORR activity of MNC catalysts –RRDE testing (NEU)

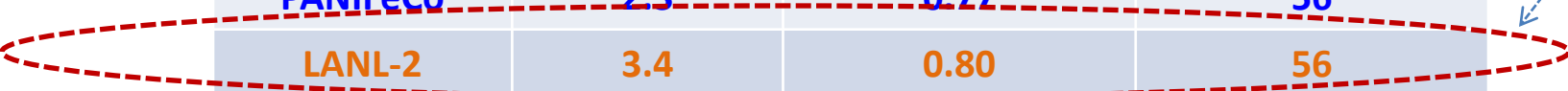


0.1M HClO₄, 0.6mg/cm² on 0.247cm² GC, RT, 1600rpm

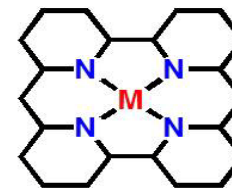
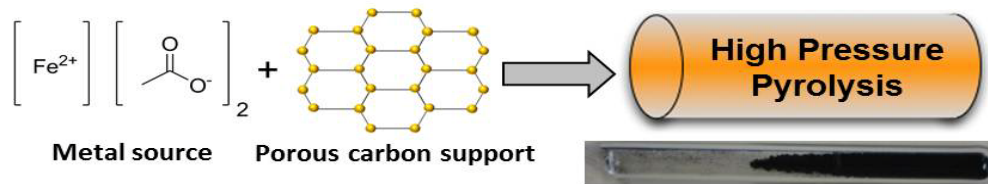


	I at 0.8[V] [mA/cm ²]	E _½ [V]	Tafel Slops, [mV/dec]
UNM Fe-AAAPyr	2.5	0.78	63
PANIFeCo	2.3	0.77	56
LANL-2	3.4	0.80	56
PVAGFe	2.2	0.77	60
PEIbFe	1.87	0.77	65

Highest ORR onset potential observed

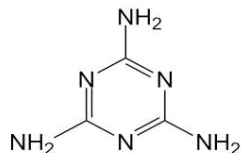


What about Durability



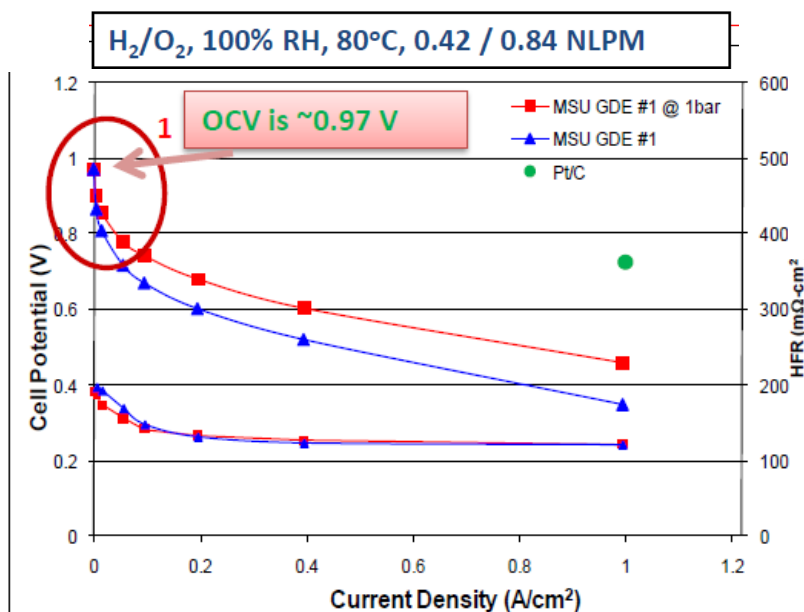
Metal-functionalized pyridinic carbon (Proposed catalytic site)

+
N precursor



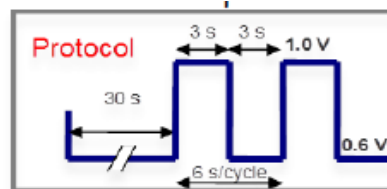
Melamine (N/C - 2.0)

Fuel Cell data - Nissan Tech. Center

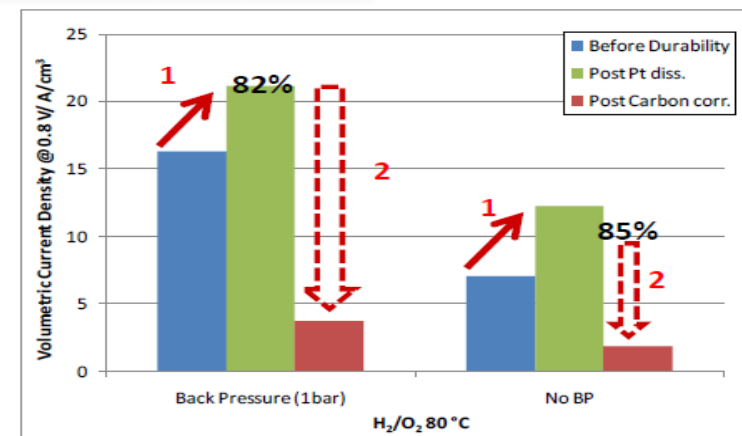
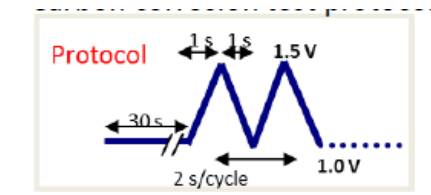


- GDEs were prepared for Melamine based catalyst using NTCNA spray system.
- MEAs were prepared with NRE211 as the electrolyte and JMFC GDE anodes.

Catalyst durability test protocol



Carbon corrosion test protocol



Testing and Durability Measurements (MSU/NTCNA)

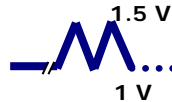
MSU-Melamine based non-PGM catalyst-Post durability performance recovery

Tests were done to recover the performance of MSU's melamine based MNC catalyst post-durability tests

➤ In-situ test results for the same have been shared during DOE AMR 2011 and ECS 220th*

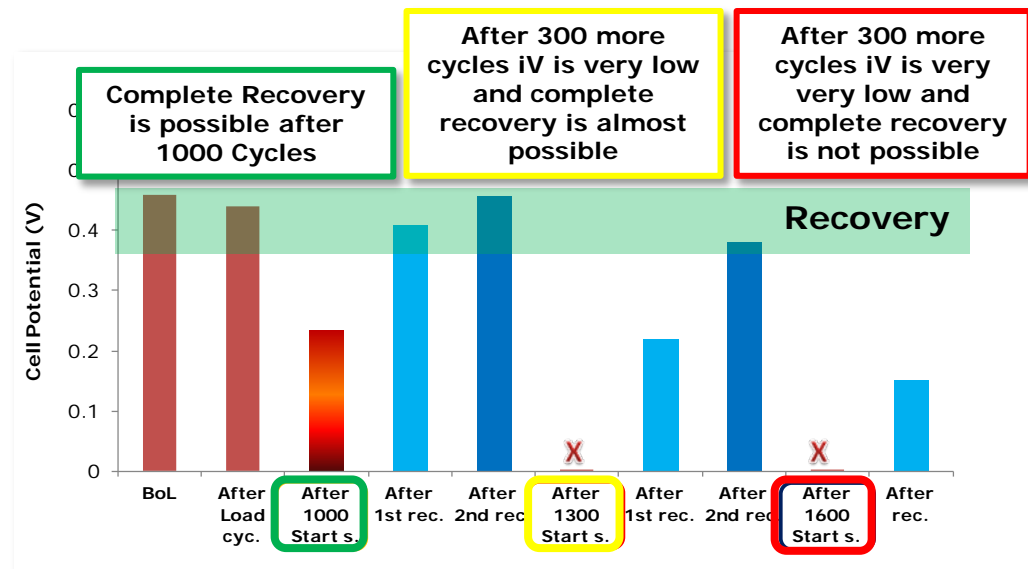
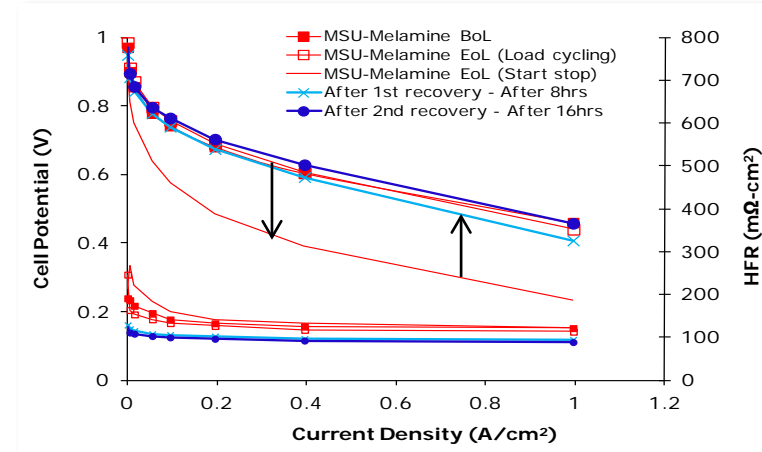
✓ During the End of Life (EoL) iV performance check (after Start-Stop test), an increase in OCV values was observed

Nissan Start-stop Protocol (1000 cycles std)



✓ Additional experiments (Post Mortem Conditioning) were performed to further investigate this phenomena and to explore an effect of surface oxide removal on partial performance recovery

✓ Complete recovery was observed after 1000 & 1300 cycles however after 1600 total cycling, MSU catalyst may reach the "not recoverable point" this is the point where there might not be enough active carbon left in order to be an effective ORR catalyst



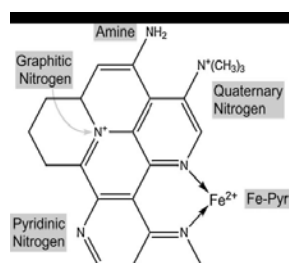
Active Site Models in the Literature for Non-PGM Catalysts

Active sites structure derived from experimental studies

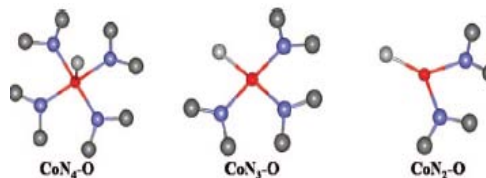


Dodelet et al, 2006

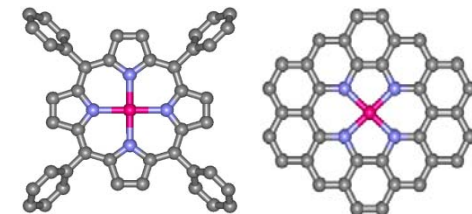
Fe-N₂ on the edge of graphene crystallite



Graphitic, Pyridinic, Pyrrolic forms of Nitrogen present
Artyushkova et al, 2007

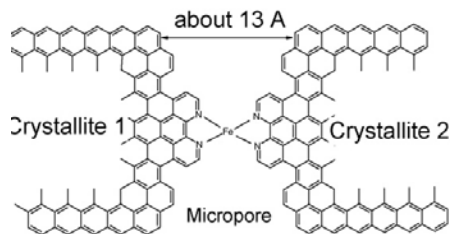


Mukerjee et al, 2008



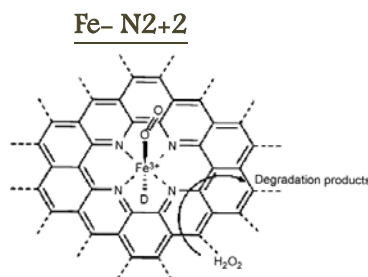
Ramaswamy et al, 2012

In-situ XAS: From porphyrin to Fe-N4-C in defective pockets of graphitic surface



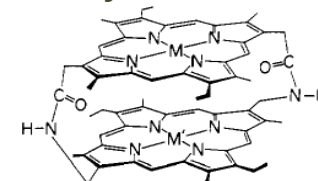
Dodelet et al, 2009

MeN₄/C species embedded in carbon micropores



Shulenburg et al, 2003

*Face-to-face porphyrins
Ideal for direct 4e ORR*

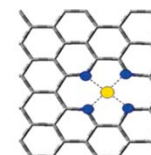


Anson et al, 1980

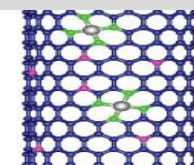
Theoretical Studies DFT calculations

- ❖ Metal coordination to nitrogen required for high activity
- ❖ Strong correlation between N-pyridinic and ORR activity

- ❖ M-N₄ defect – energetically favorable over metal-less defects (DFT calculations)
- ❖ Pyridinic configurations are energetically preferred over pyrrolic



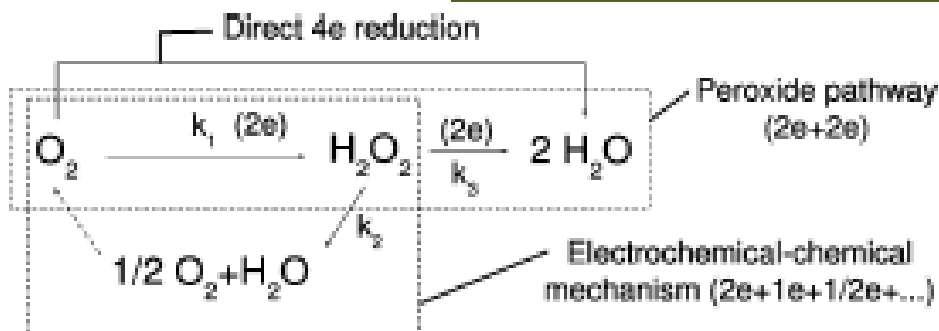
Titov et al, 2009



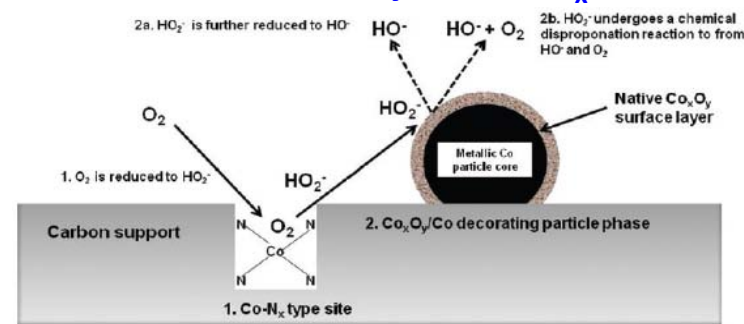
Kim et al, 2011

Mechanistic Pathways in the Literature for Non-PGM Catalysts

Direct 4e or 2x2e ORR mechanism ?

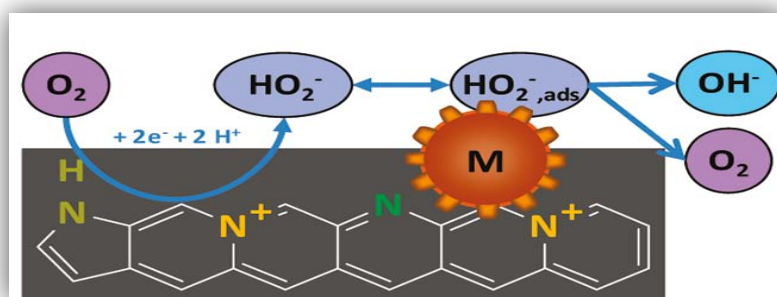


Bi-functional Theory: Metal-N_x



Atanassov et al, 2010

Bi-functional Theory: Metal-free active sites



Stevenson et al, 2011

❖ Metal-Free centers as primary active sites:

2e O₂ reduction to HO₂⁻, and

❖ Adsorption of HO₂⁻ on Metal/Metal-oxide, and further 2e reduction of HO₂⁻ to H₂O, and/or heterogenous decomposition to H₂O and O₂

➤ 2e Oxygen reduction to HO₂⁻ at primary active site - Metal-N₄, and

➤ Further electrochemical reduction of HO₂⁻ to H₂O at Metal/Metal Oxide and/or chemical decomposition

In-situ XAS/ Electrochemical studies

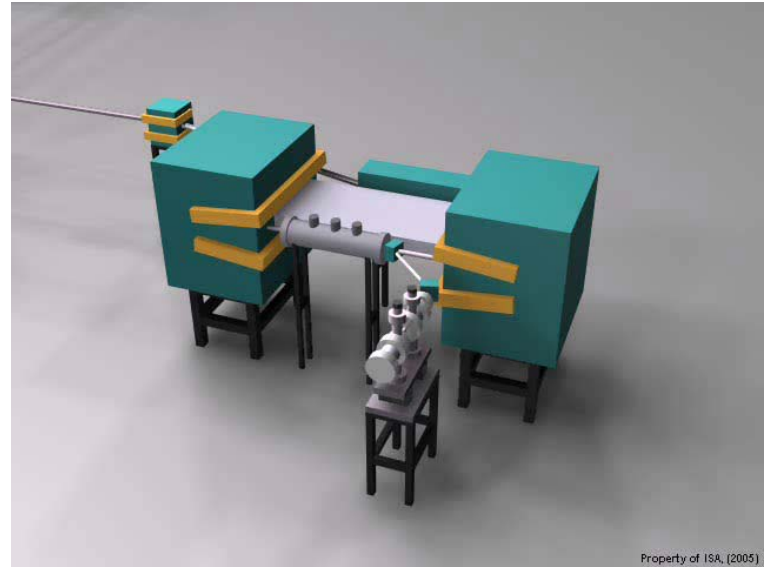
➤ Metal-N_x centers sufficient for overall 4e ORR in alkaline media:

❖ 2e O₂ reduction to HO₂⁻, and further 2e conversion to H₂O at the same Metal-N₄

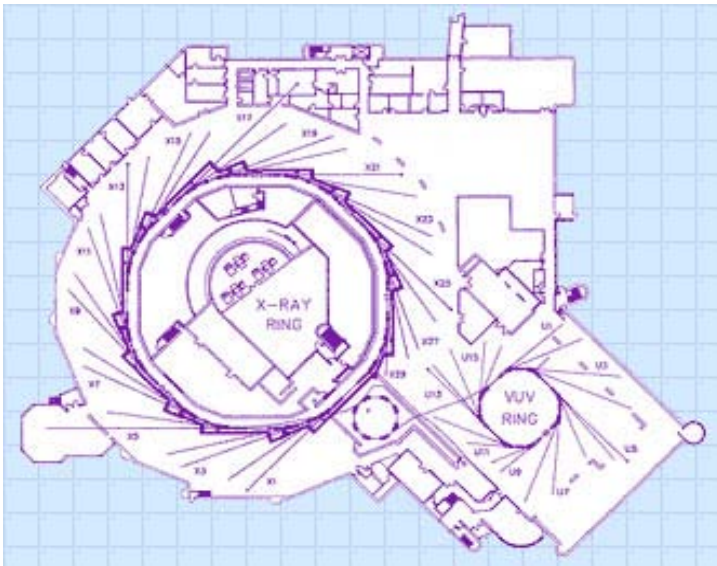
➤ In acid, Metal-N₄ not able to perform the HO₂⁻ reduction. Secondary active site needed

Ramaswamy et al, 2012

Synchrotron Spectroscopy



Property of ISA, (2005)



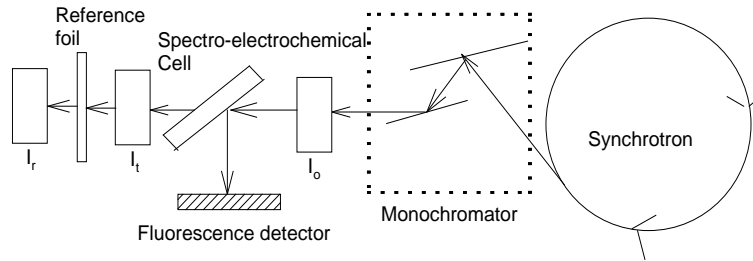
Property of ISA, (2005)

X-ray absorption spectroscopy

an element specific, core level spectroscopy

Synchrotron Advantages

- High Intensity
- Broad Spectral Range
- High Polarization
- Flux > 10¹⁰ photons/s
- Natural Collimation



EXAFS, single backscatter

Physical Basis

Determination of short range atomic order (bond distance, coordination number, Debye Waller factor etc.,)

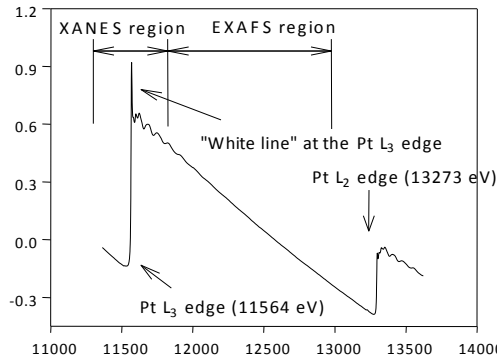
XANES, multiple scattering

Physical Basis

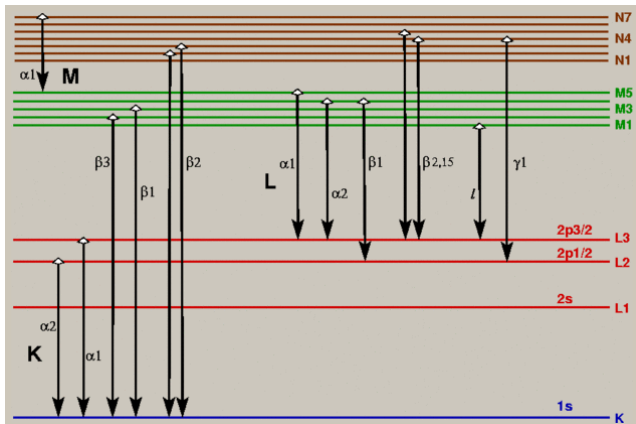
- Determination of oxidation state and coordination symmetry
- Electronic Structure
- Extent of Corrosion

$$E_{\text{photoelectron}} = E_{\text{xray}} - E_0$$

$$\mu x = \ln(I_0/I_t)$$



- N** – Coordination Number
- R** – Interatomic Distance (Å)
- σ²** – MSRD (Debye-Waller)
- f(k)** – Amplitude
- δ(k)** – Phase



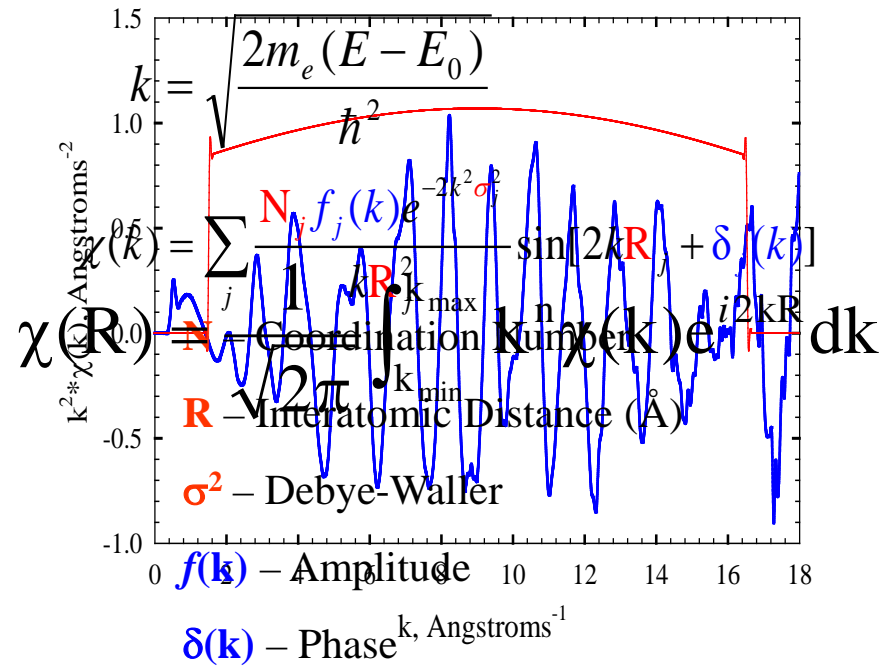
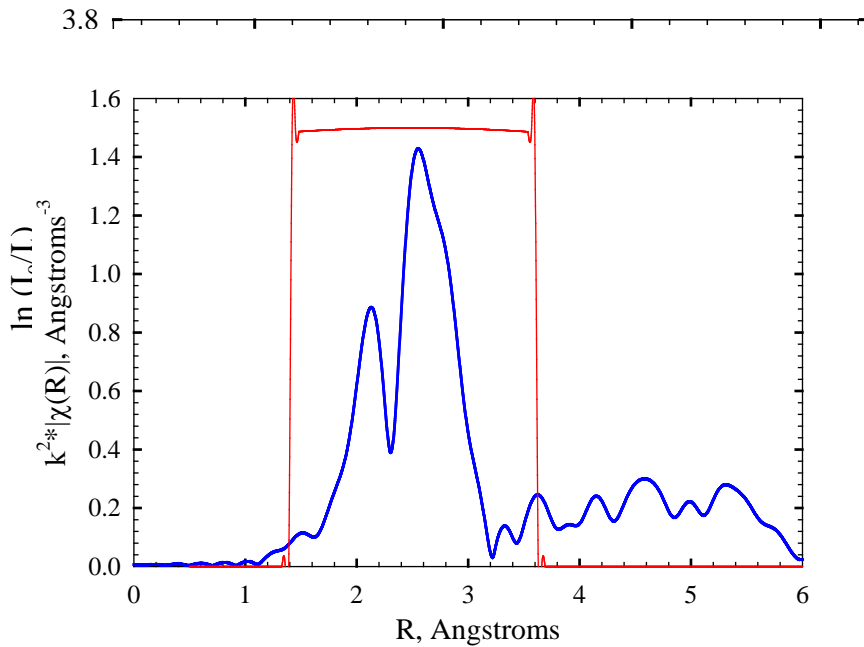
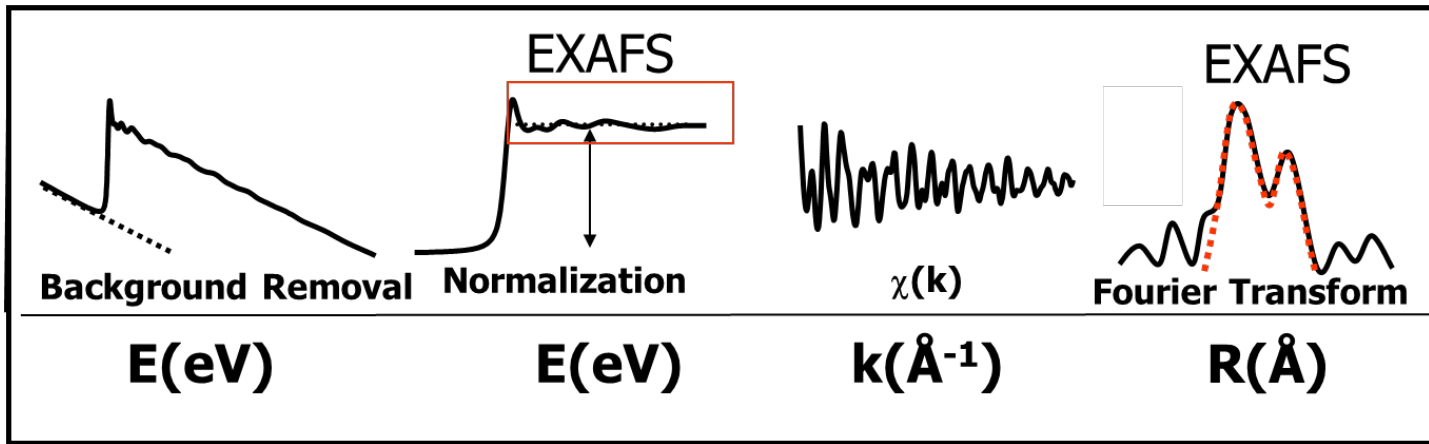
Detection:

- State-of-the-art 13 element Ge array detector
- Gas ionization chambers
- Photomultiplier tubes
- 14K Cryostat

$$E_{\text{xray}} = \frac{hc}{\lambda}$$

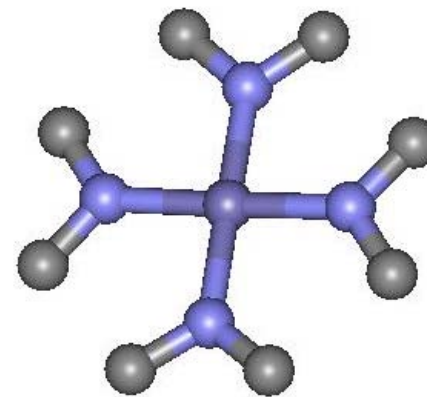
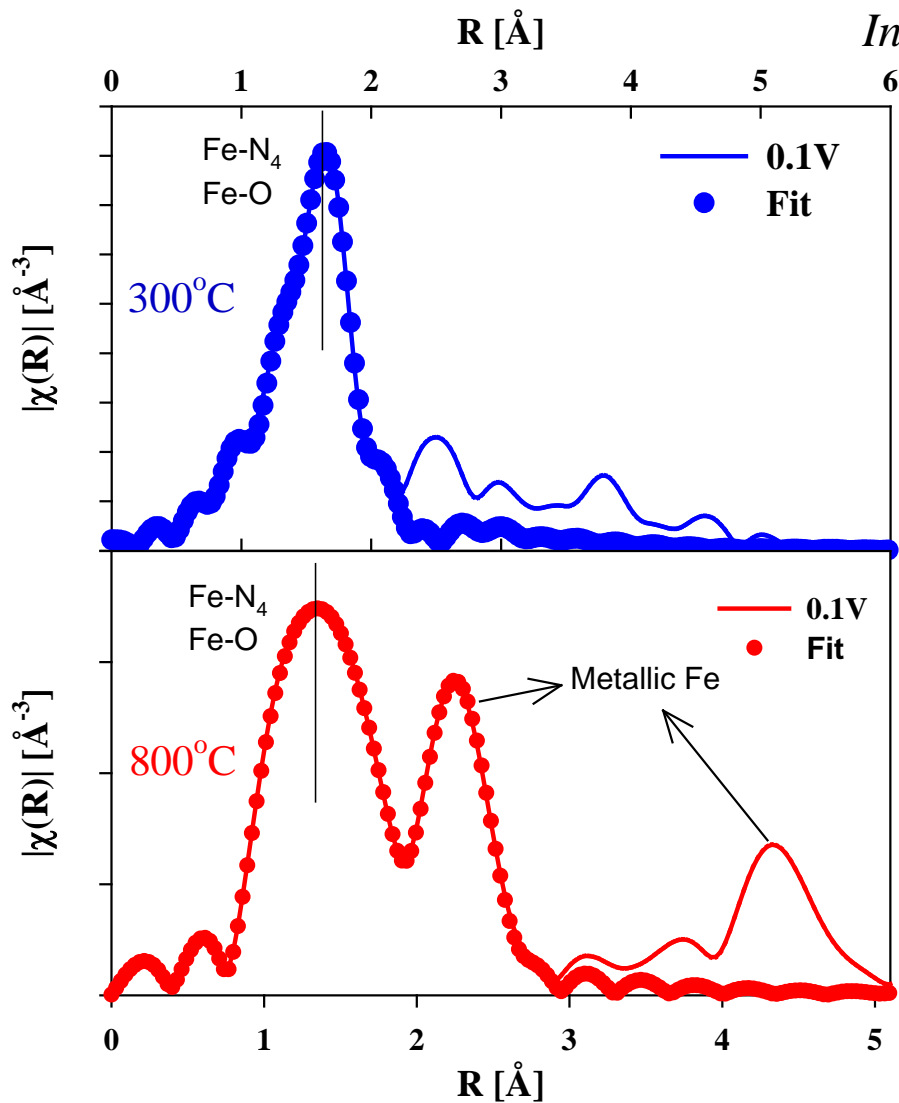


Data analysis 1: EXAFS





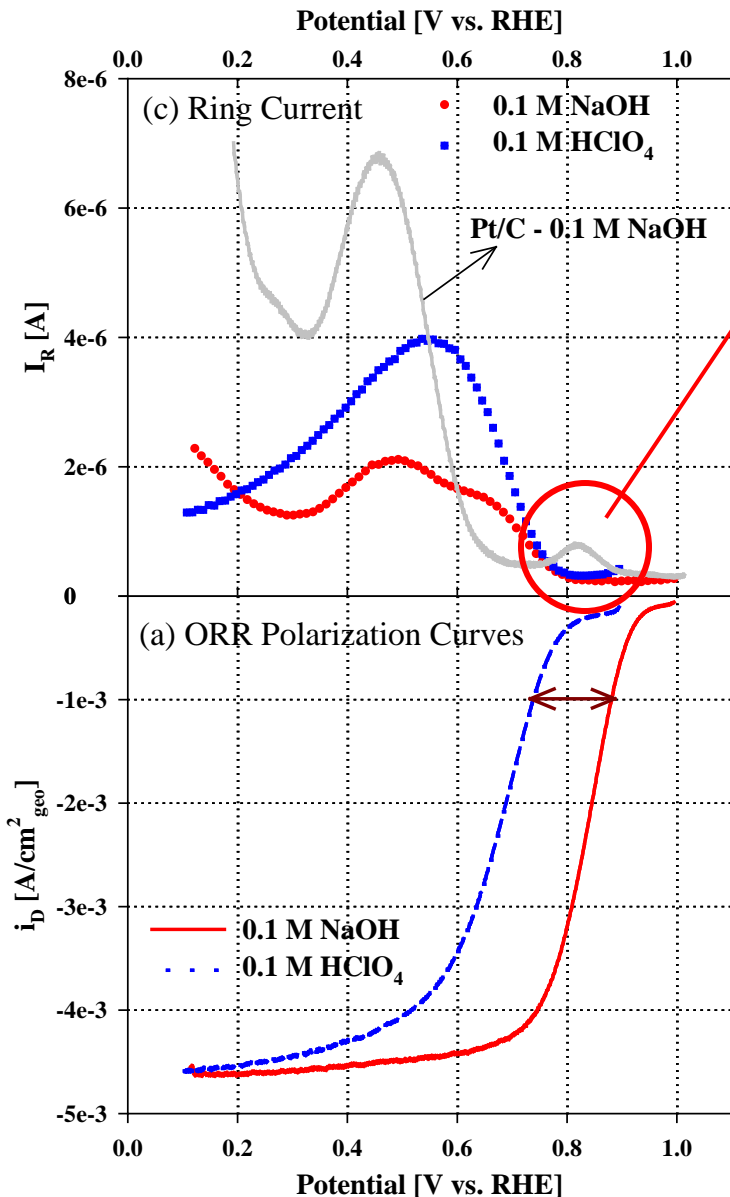
In situ 0.1M NaOH electrolyte @ 0.1 V vs. RHE



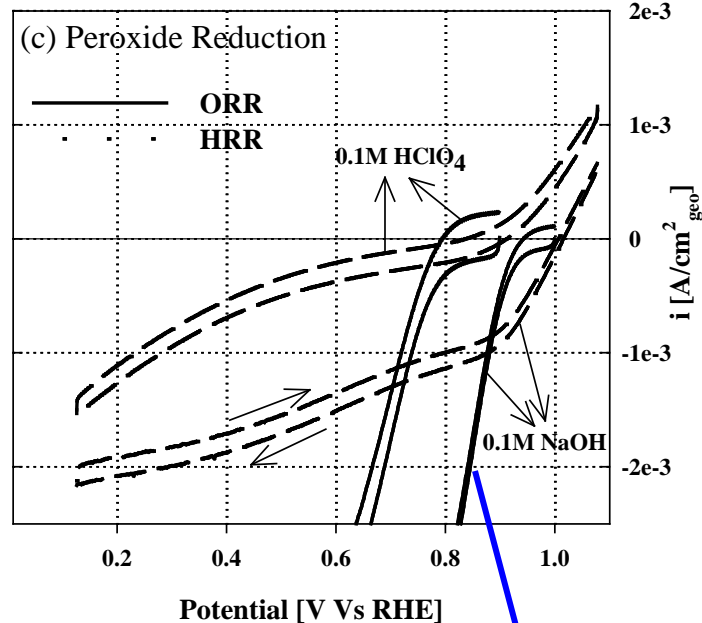
	Fe-N Coordination Number	Fe-N Bond Length [Å]
300°C	4.00	1.996
800°C	4.00	1.976

O₂ Reduction Activity – Acid versus Alkaline Perspective

Iron-Porphyrin/Carbon
 Pyrolyzed – 800°C
 100 μg/cm² Loading

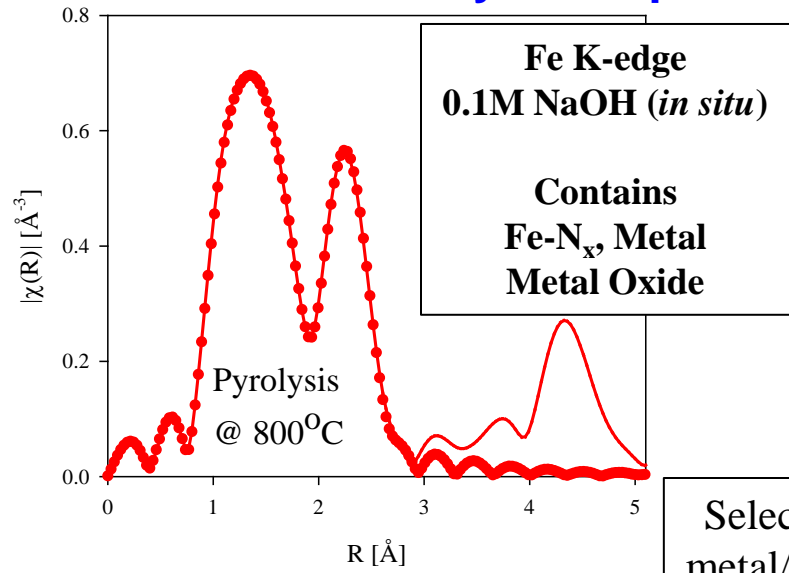


**No Outer-Sphere Process
 on Pyrolyzed Fe-Porphyrin**

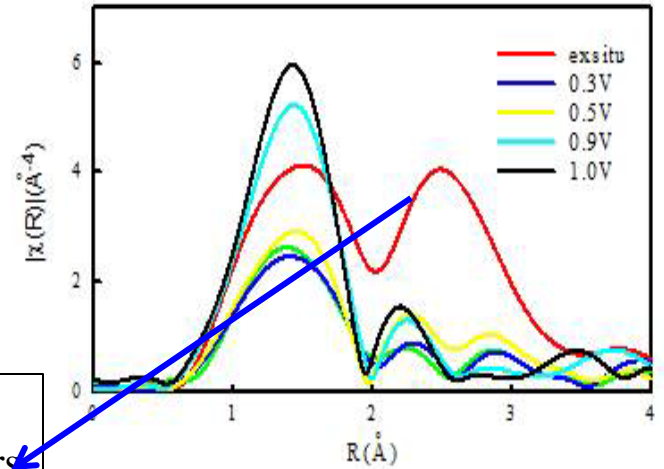


Peroxide intermediate is more stable on the active site in alkaline media

In situ Extended X-ray Absorption – Fe-N_x Short Range Structure

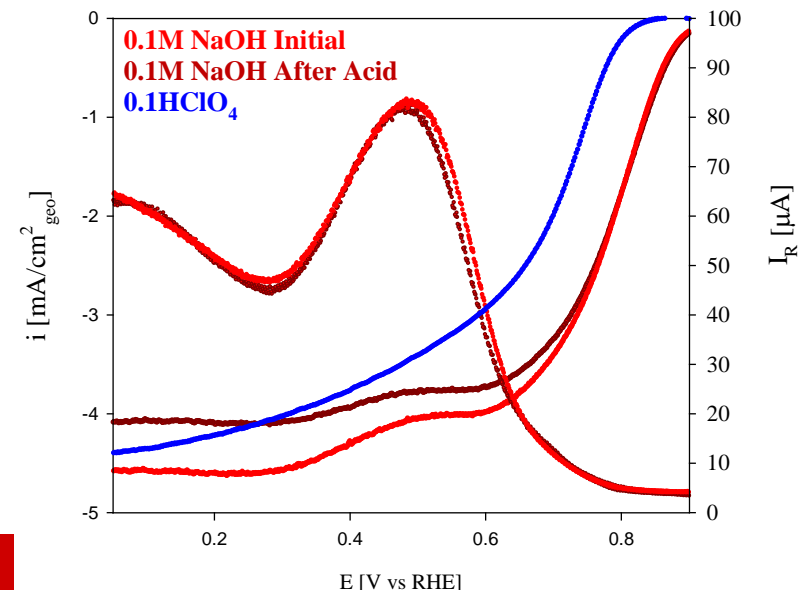
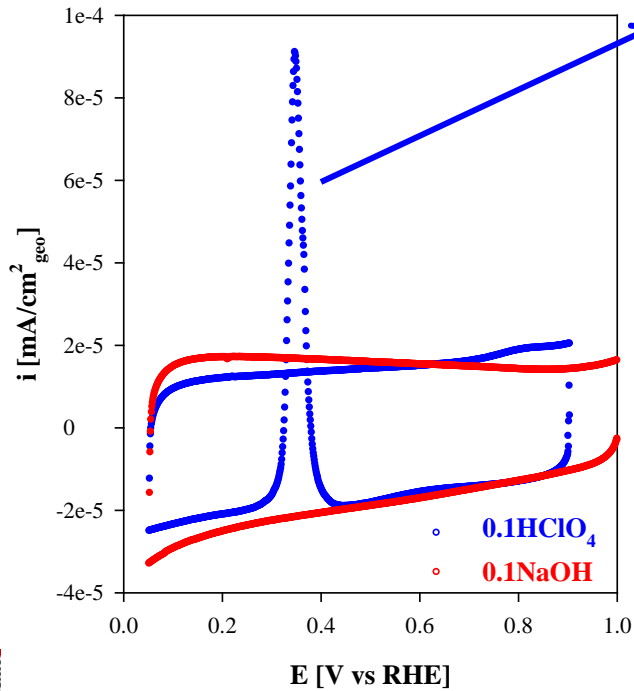


Fe-Porphyrin HT800°C
In situ 0.1M HClO₄ electrolyte

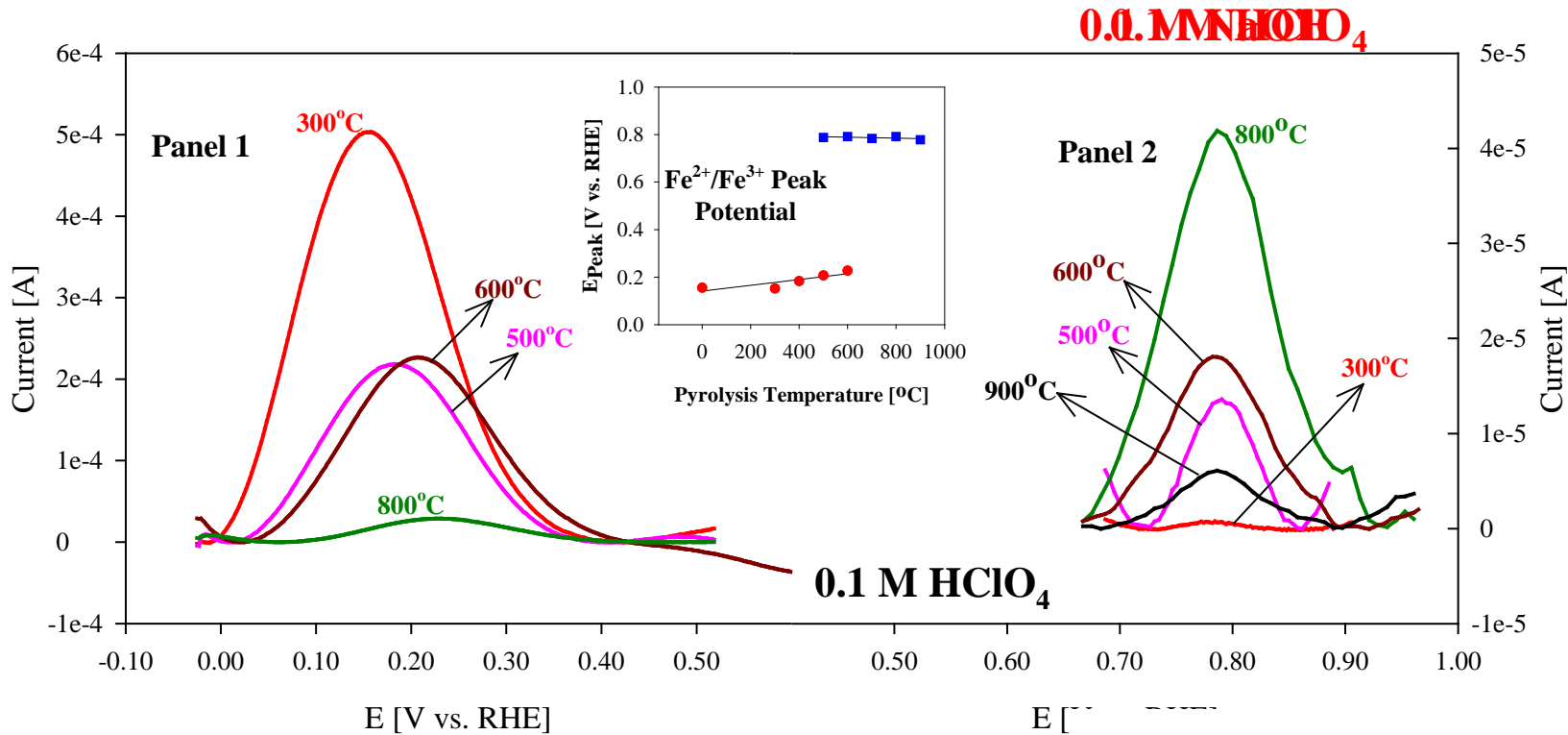


Selective dissolution of metal/metal oxide clusters in acidic media confirmed by EXAFS

No Loss in activity after removal of metal/metal oxide clusters



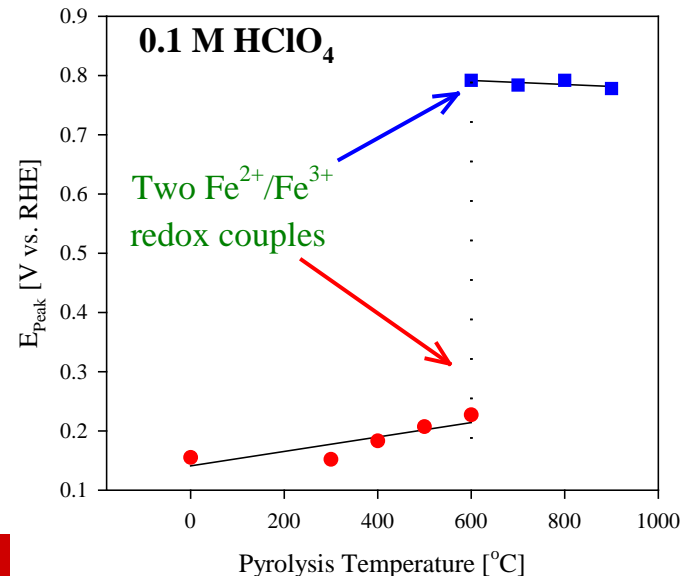
Pyrolyzed Fe-Porphyrin on Carbon – Square wave Voltammetry



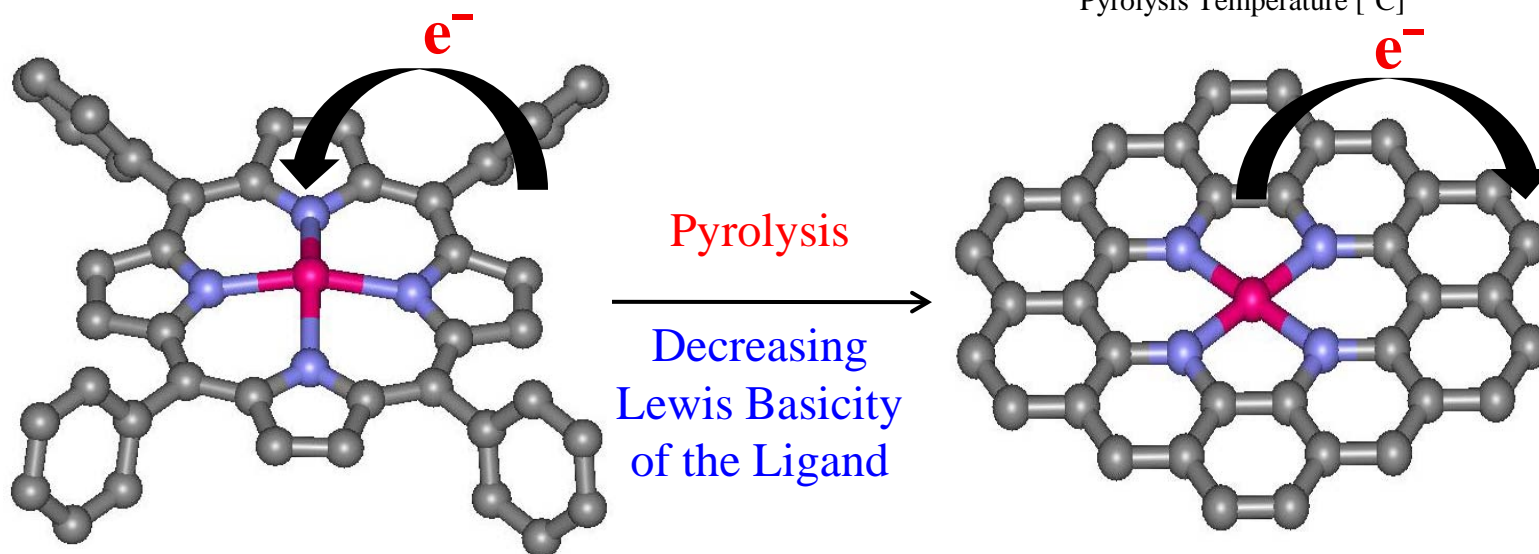
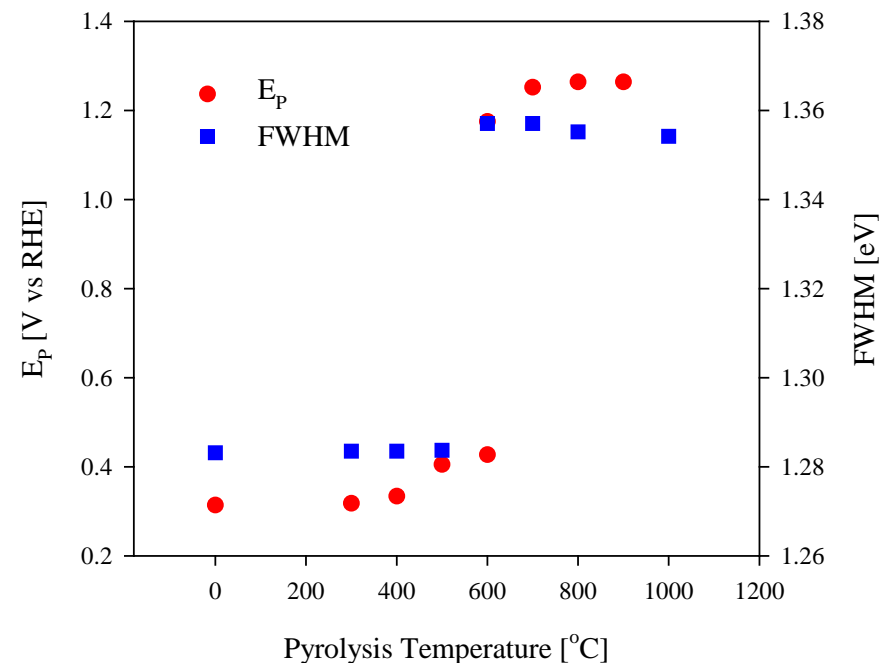
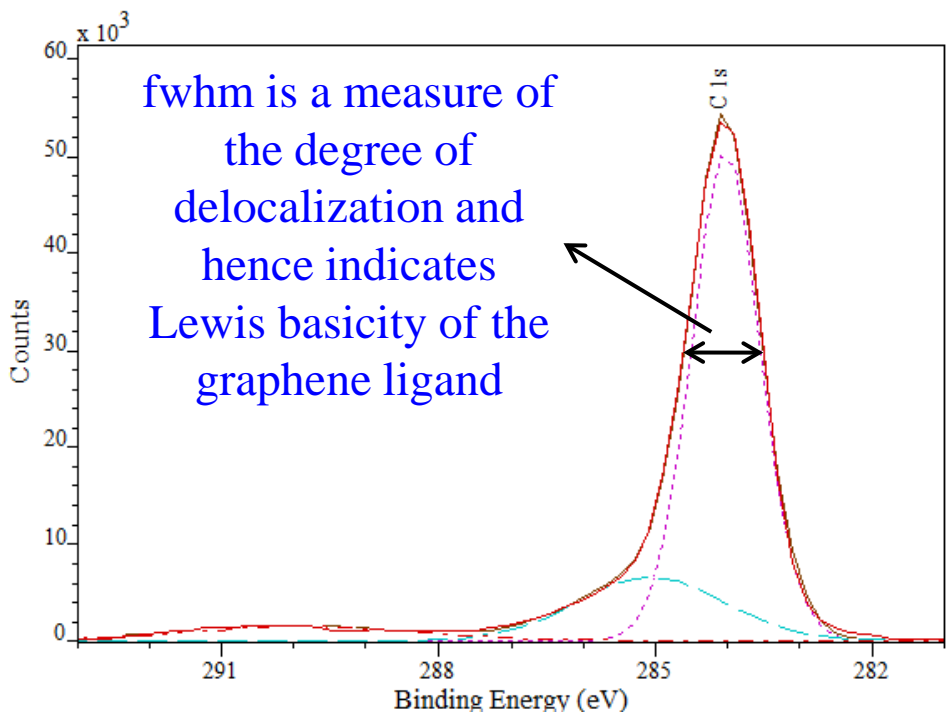
In alkaline media:

Dramatic anodic shift in the Fe²⁺/Fe³⁺ to 0.85V redox potential upon pyrolysis at 600°C

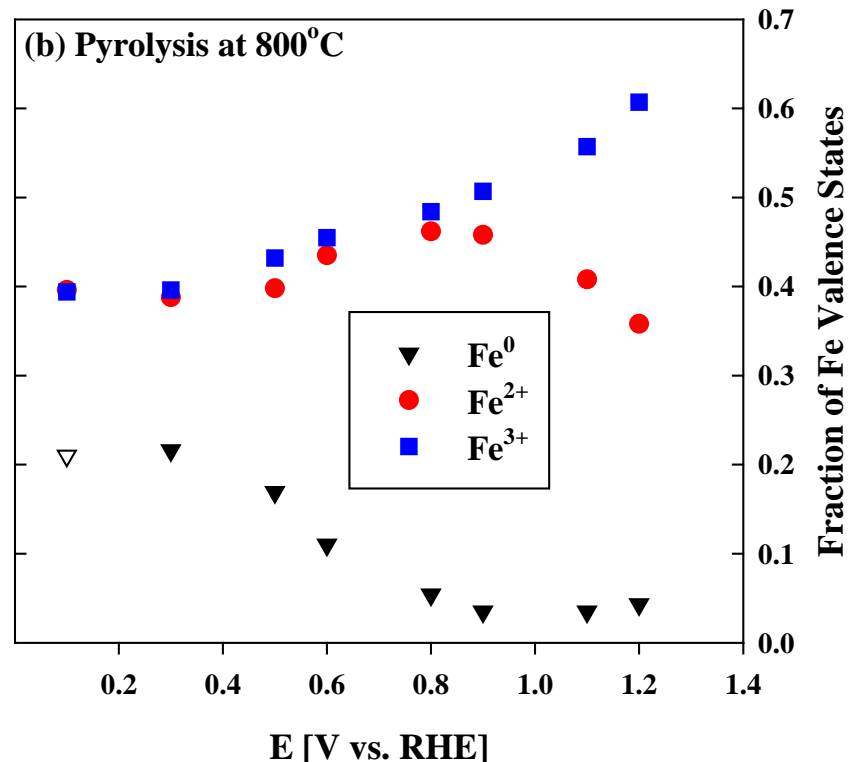
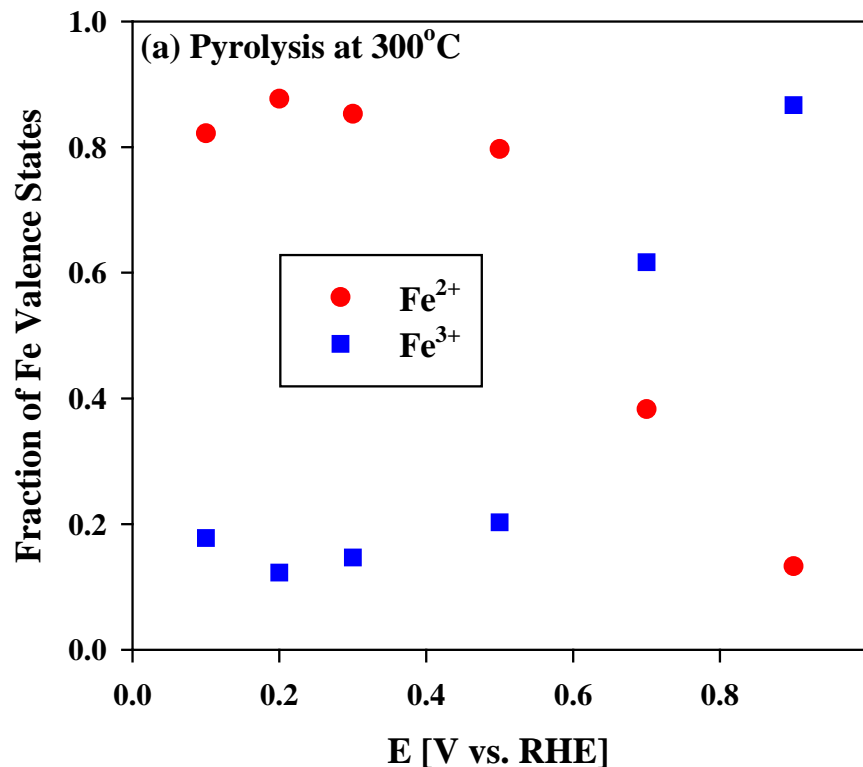
- In acidic media redox potential shifts only to 0.8 V
- Its one reason for higher overpotential in acidic media



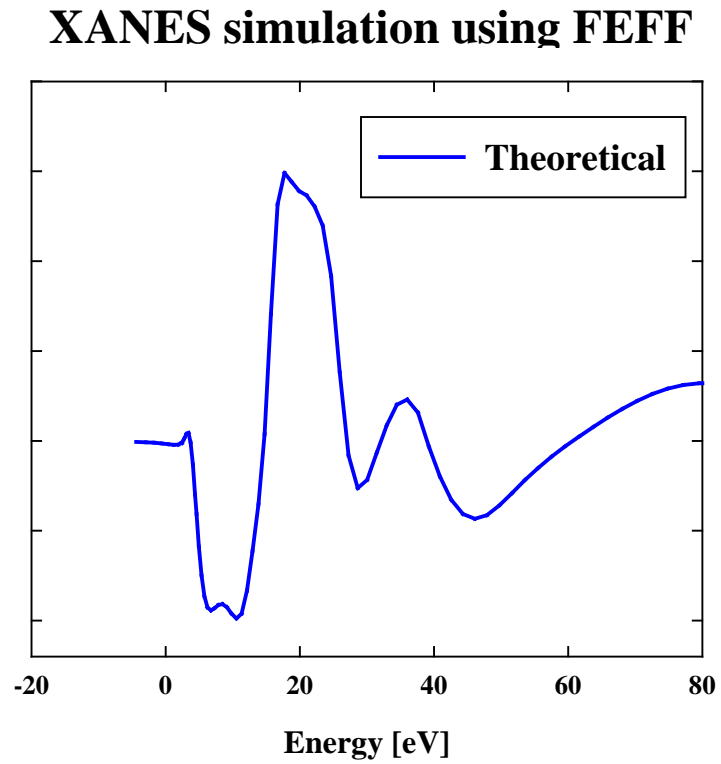
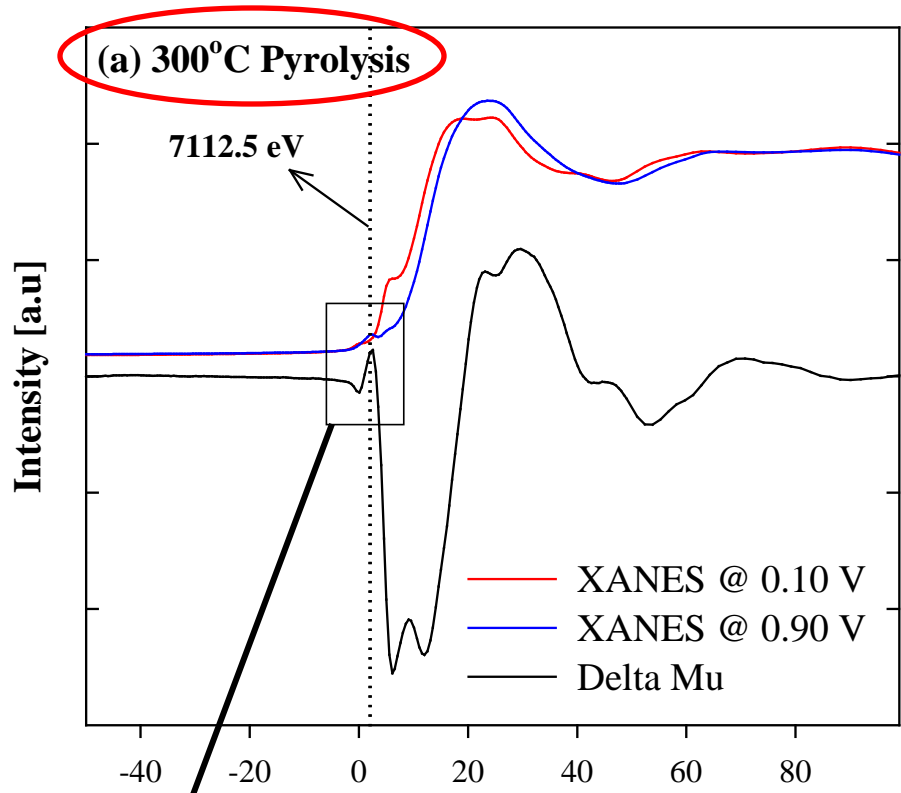
Effect of Lewis Basicity of Ligand on Redox Potential



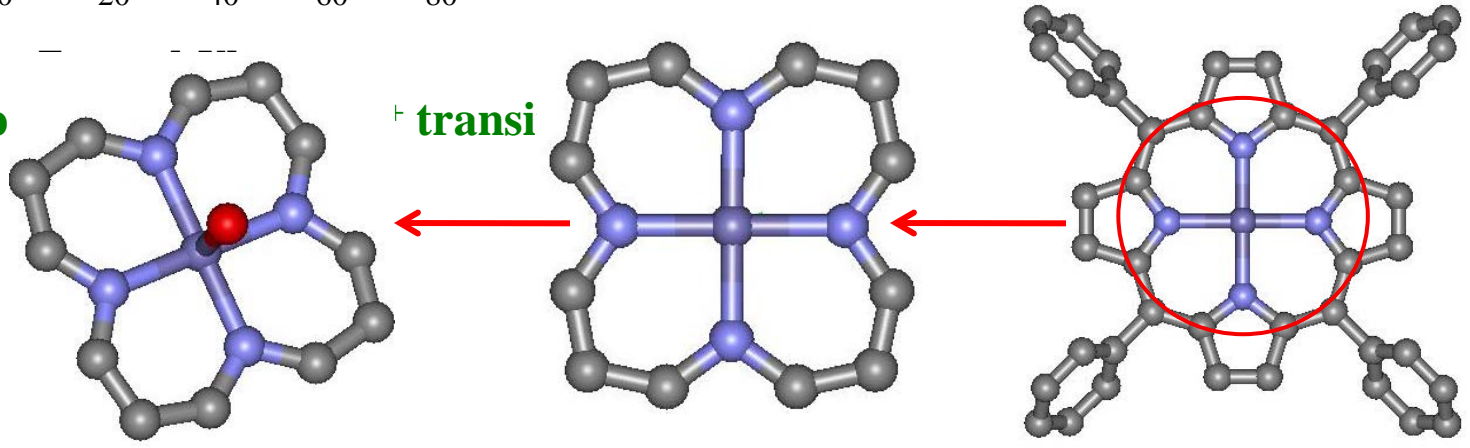
Linear Combination Fitting Analysis of various oxidation states of Fe under insitu conditions

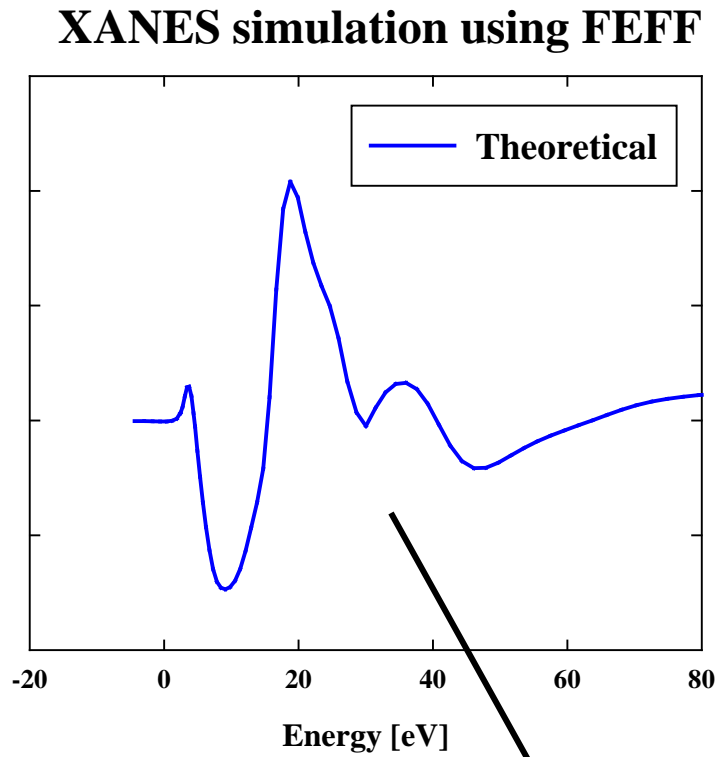
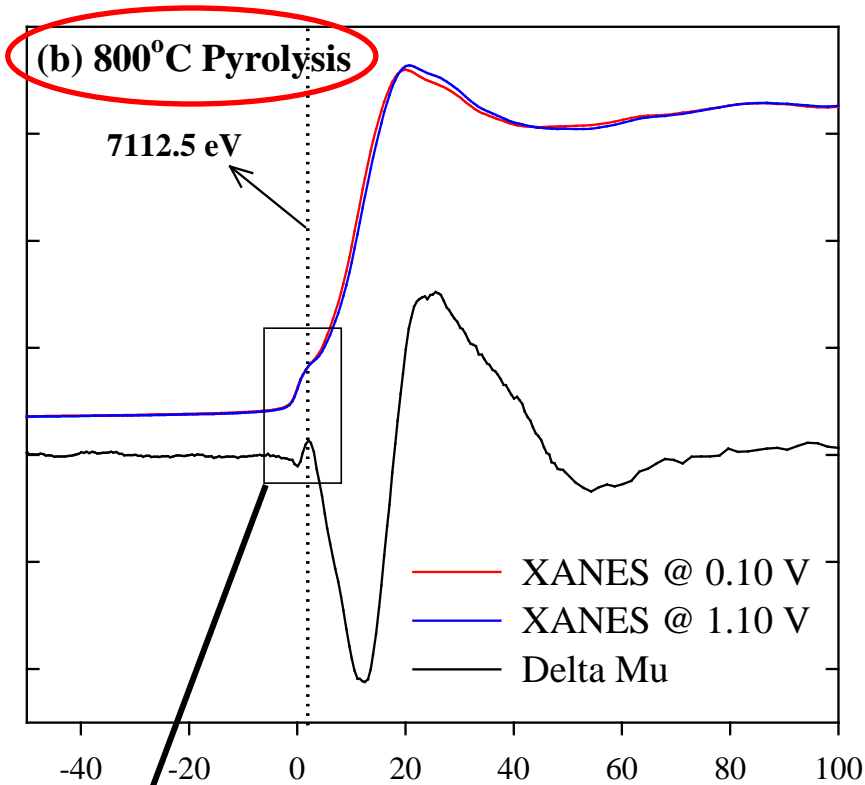


➤ After 800°C pyrolysis, XANES indicates the shift in Fe^{2+/3+} transition to higher potentials

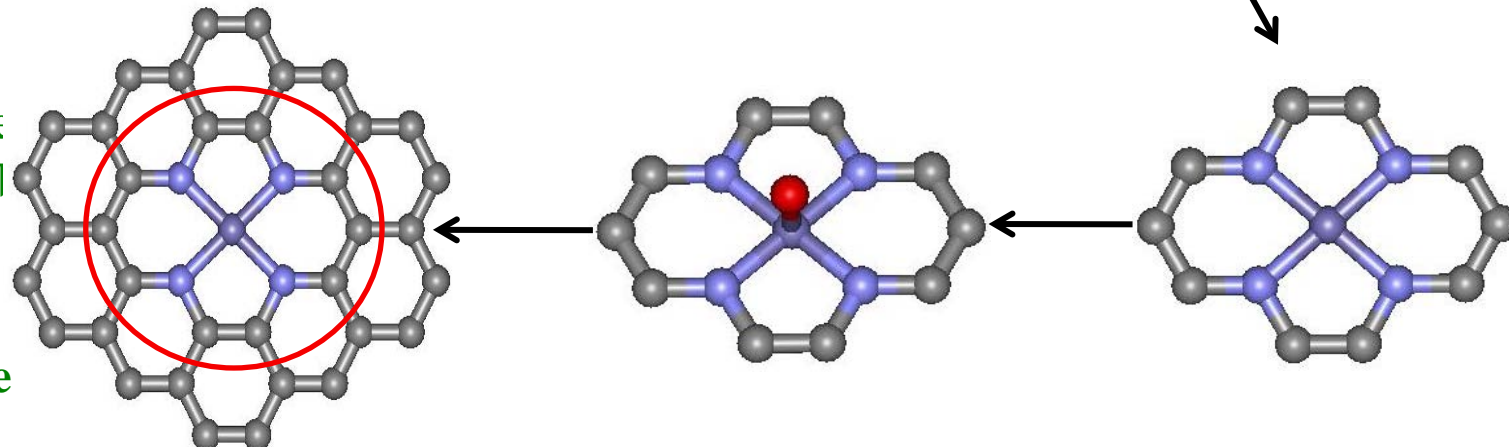


Delta Mu after
pyrolysis
 FeN_4 structure is
preserved in the
macrocyclic cavity

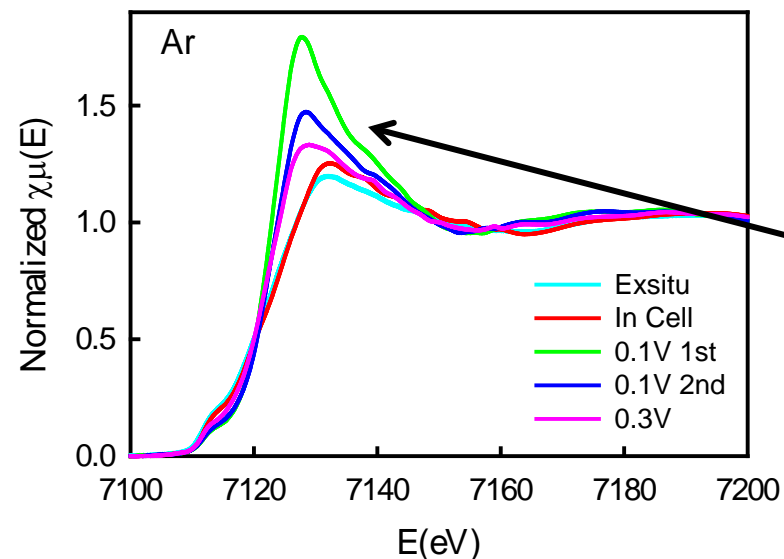




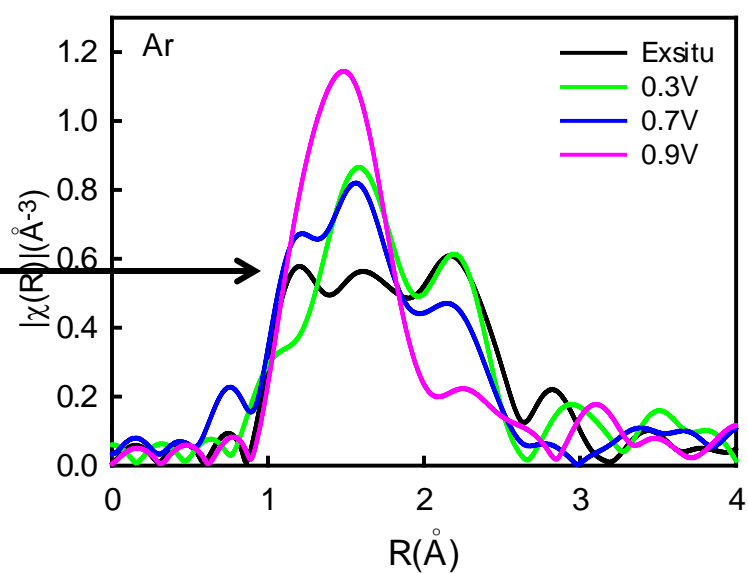
After 800°C
Fingerprint for Fe
pyrolysis
active site is
still of
reminiscent of
divacant defective
regions on graphite



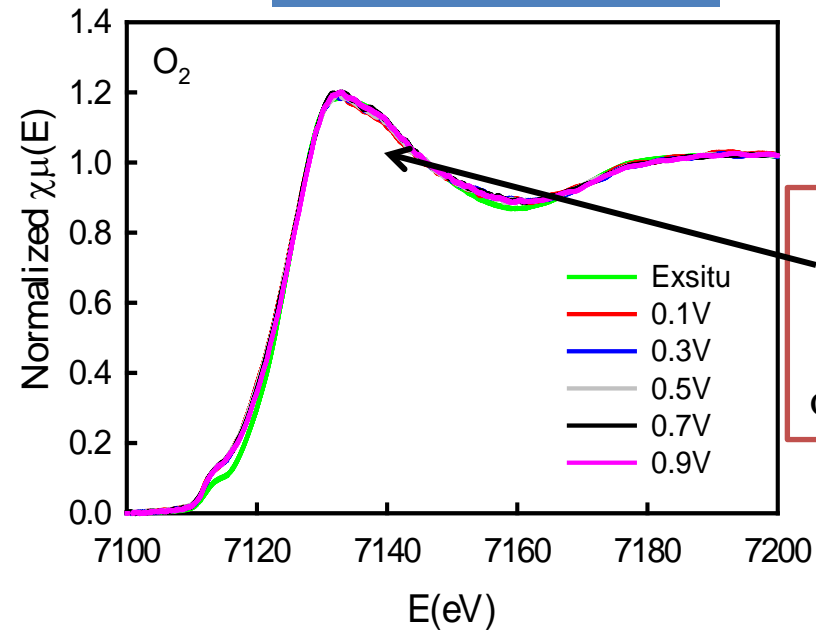
PANI_FeCo (LANL)



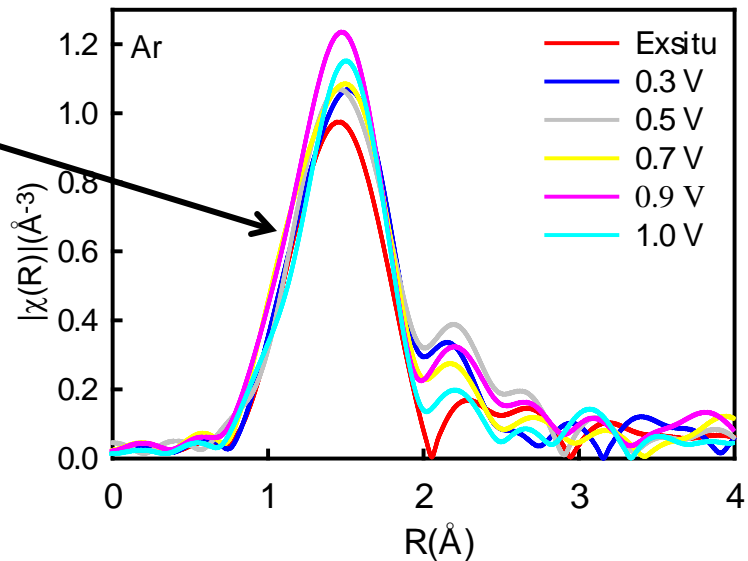
LANL PANI/FeCo



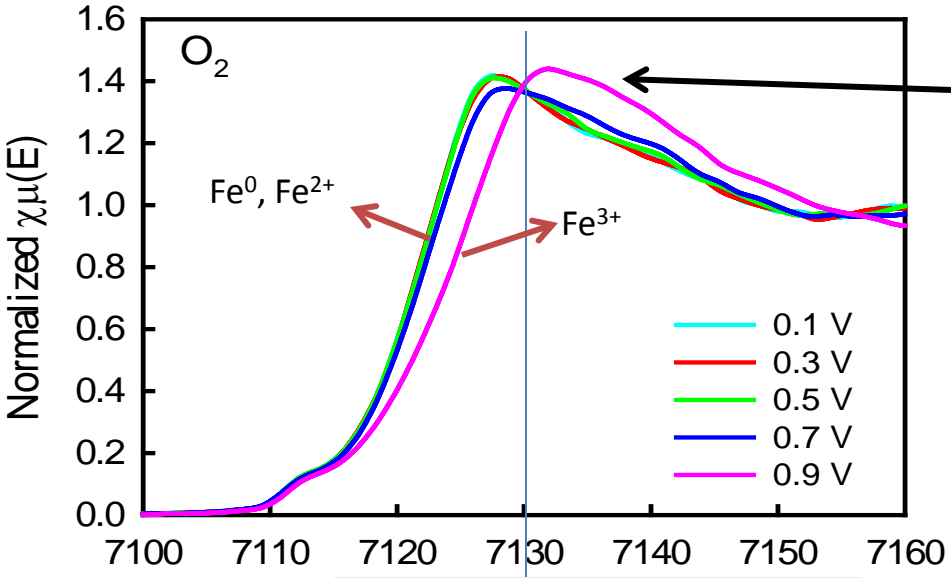
LANL-2



LANL-2



PANI_FeCo (LANL)

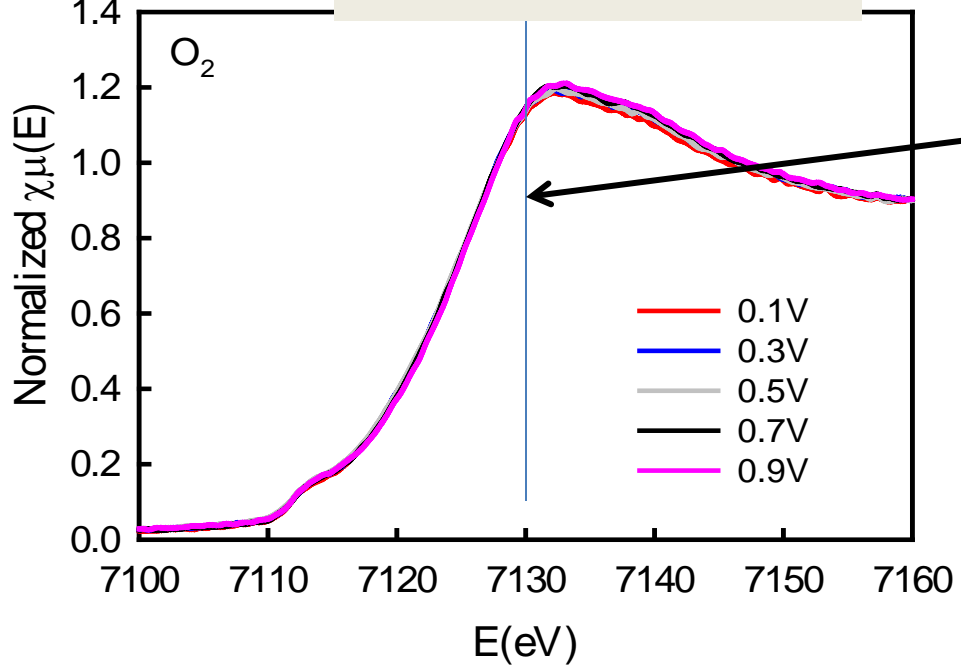


A significant shift at 0.9 V

LCF	Fe	FeO	Fe ₂ O ₃
exsitu	40%	0	22%
0.3 V	19%	23%	17%
0.9 V	5%	5%	37%

A large amount of Fe NPs initially.

LANL-2

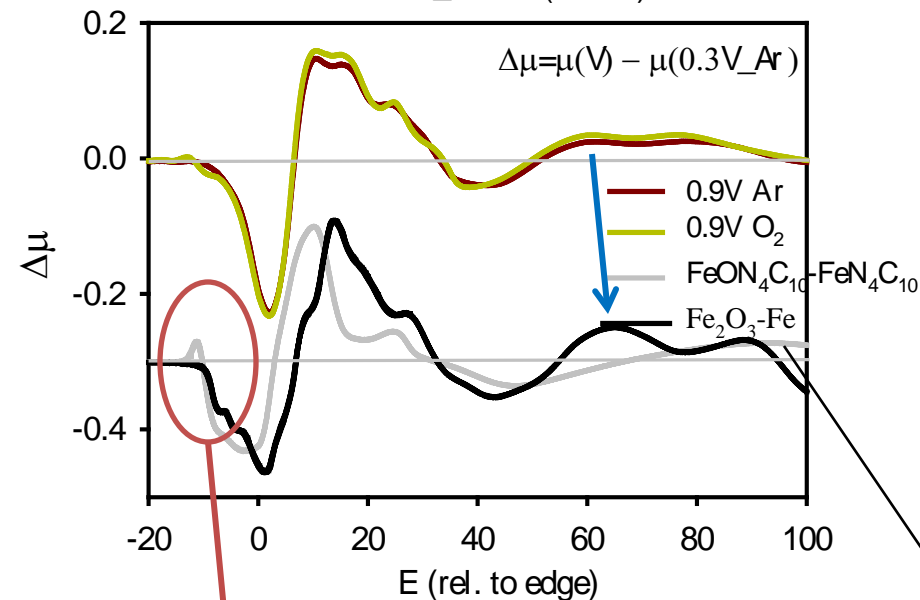


Non-significant shift observed, spectra show the domination of Fe³⁺.

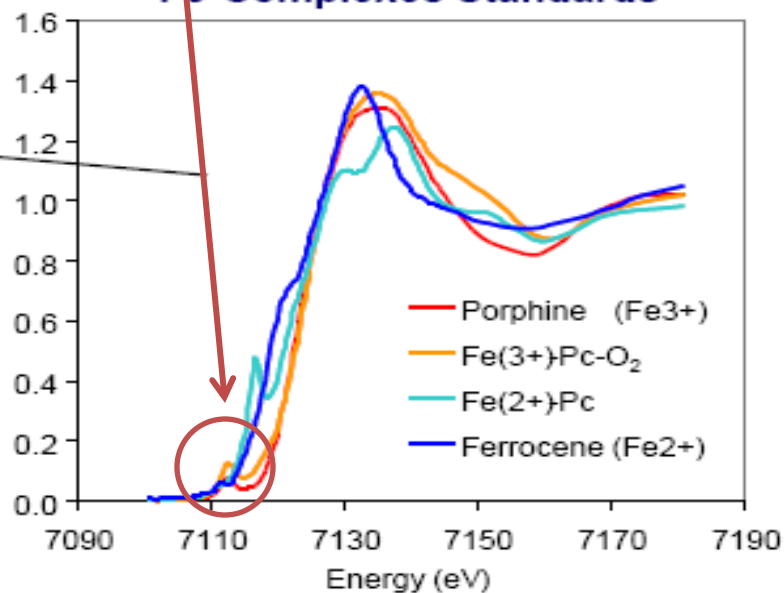
LCF	Fe	Fe ₂ O ₃
exsitu	0%	16%
0.3 V	7%	25%
0.9 V	11%	22%

No Fe NPs initially.

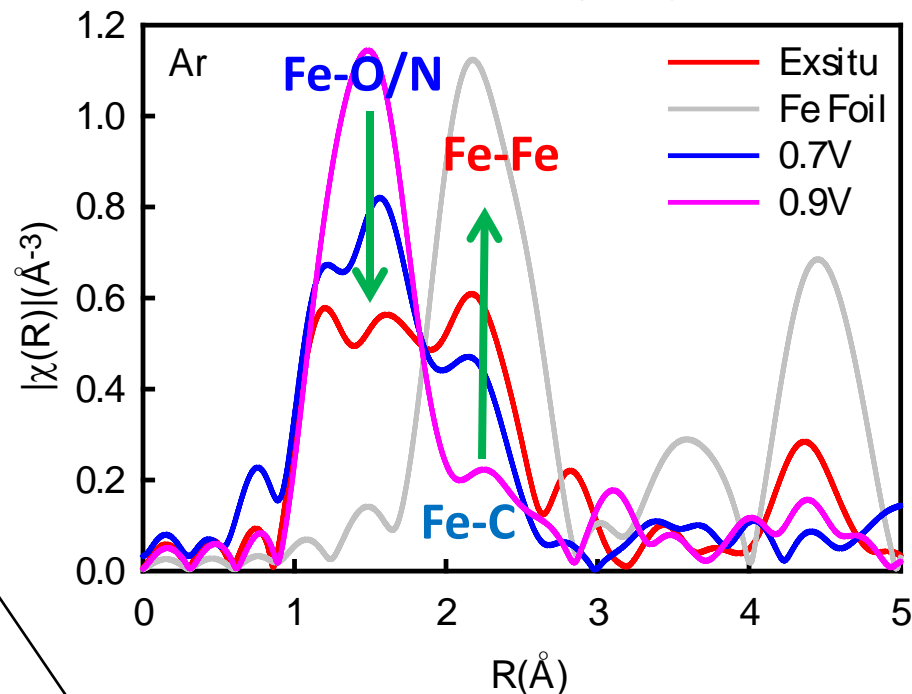
PANI_FeCo (LANL)



Examples of Fe-Complexes Standards



PANI_FeCo (LANL)



$$\begin{aligned} \Delta\mu &= \mu(0.9V) - \mu(0.3V) \\ &= (FeN_4 + Fe_2O_3) - (FeN_4 + Fe) \\ &= Fe_2O_3 - Fe \end{aligned}$$

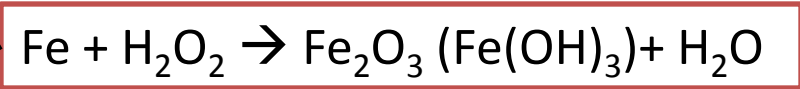
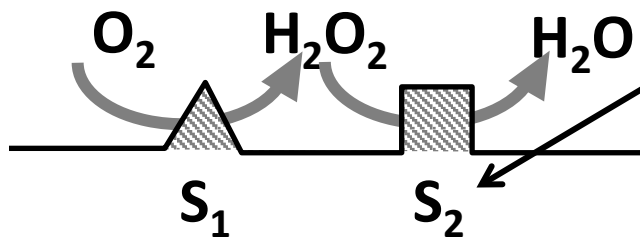
DFT (UNM): In acidic medium, H₂O₂ does not bind on Fe/Co-N₄.

The significant shift at 0.9 V is caused by oxidation of Fe NPs (and/or FeO) but not FeN₄.

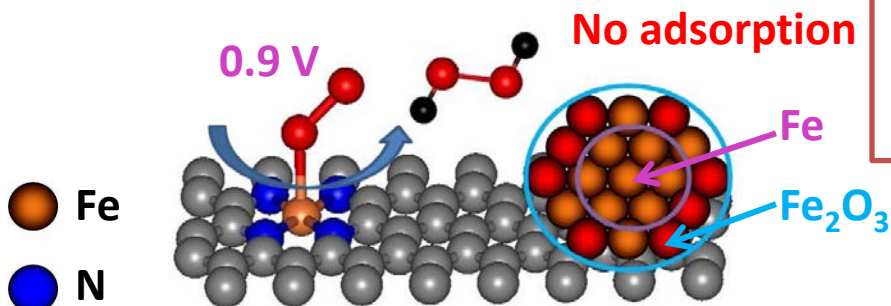
Proposed mechanism

for LANL PANI/FeCo and others

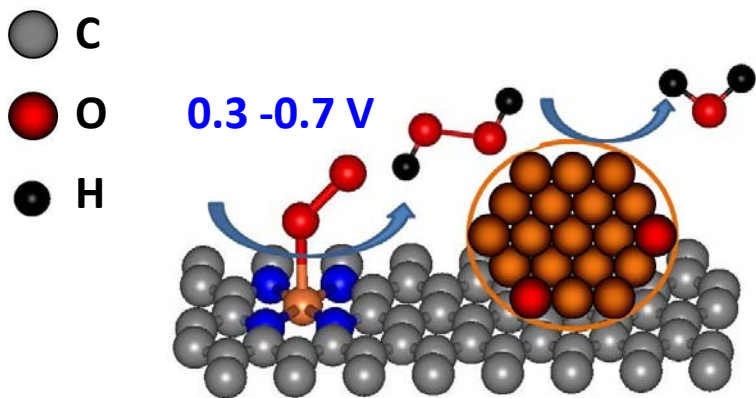
Dual site consequential:
2 x 2e- bifunctional mechanism



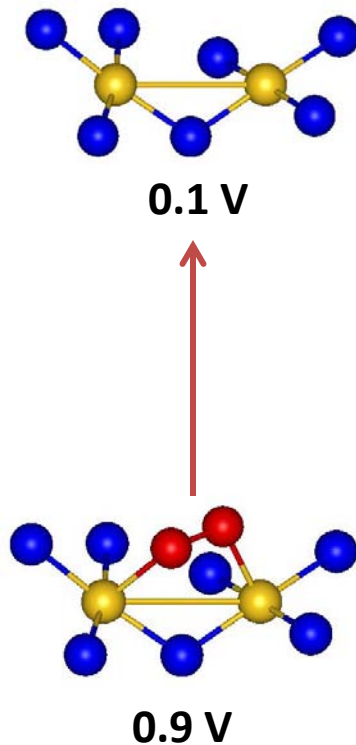
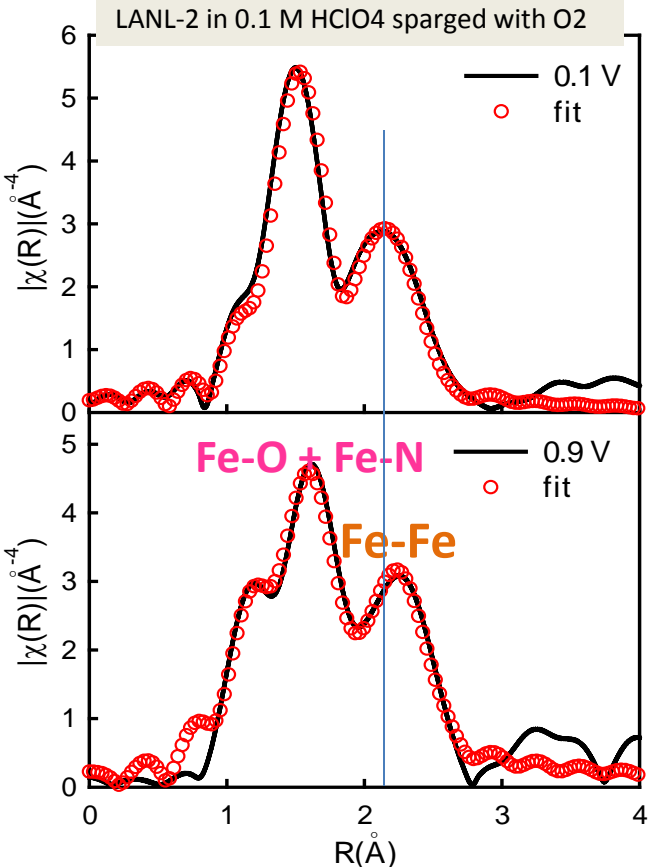
0.9 V: stabilized Fe₂O₃ inhibits the second step*
* Fe₂O₃ is very stable and cannot be dissolved sufficiently in acid to form Fe²⁺ or Fe³⁺. On the contrary, FeO or Fe₃O₄ can be dissolved in the reduced state.



Further experiments (XPS) to clarify the content of the material before and after the cycling to confirm the transition between Fe and Fe₂O₃.



Multi-component nature make EXAFS analysis of Fe K-edge spectra virtually impossible

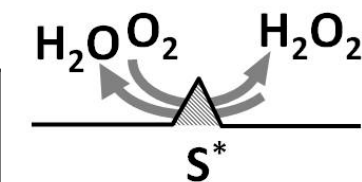
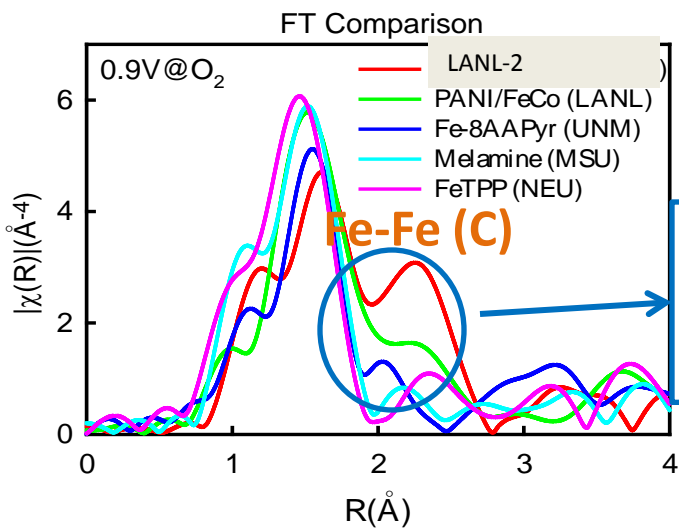


Under O ₂		FeN	FeFe	FeO
CN	0.1V	4.1±0.4	1.4±0.3	0
	0.9V	4.5±1.0	1.2±0.3	1.3±0.4
R (Å)		2.01±0.01	2.54±0.01	1.84±0.02

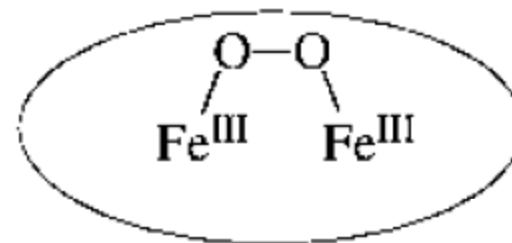
This distance is not from Fe NPs because:

1. Non-significant edge shift.
2. No Fe NPs initially.
3. No increase in the first peak, but slight increase of Fe-Fe BD at 0.9 V.
4. Sustained Fe-Fe peak at 0.9 V.
5. The better performance.

Thus it suggests the formation of the bridged structure, which favors the release of H₂O₂ and the 4-electron reduction pathway.*



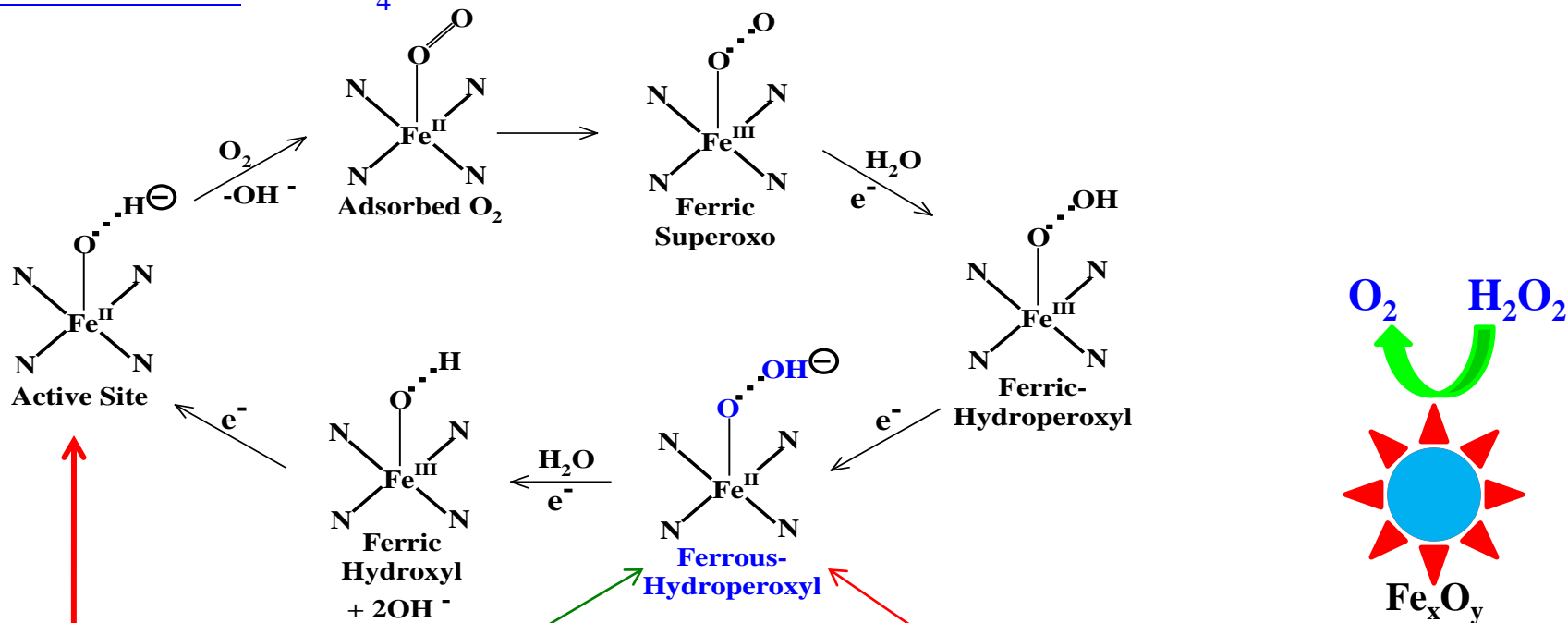
Lack of the Fe-Fe bond at 0.9 V of other samples suggest the bifunctional mechanism.



*Jungwon Hwang, et al., Science 287, 122 (2000)

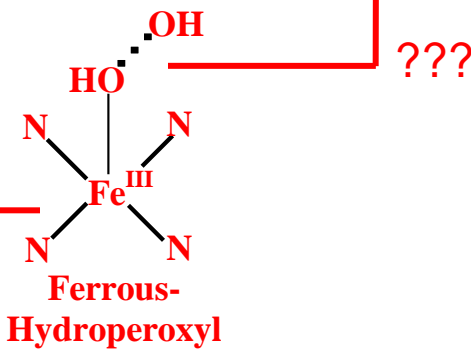
Oxygen Reduction Mechanism on Fe-N₄ Sites

In Alkaline Media – Fe-N₄ sites are true 4e⁻ sites



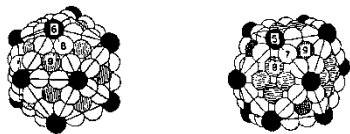
Frumkin-type electrostatic double-layer effect stabilizes peroxide intermediate in alkaline medium

In Acidic Media

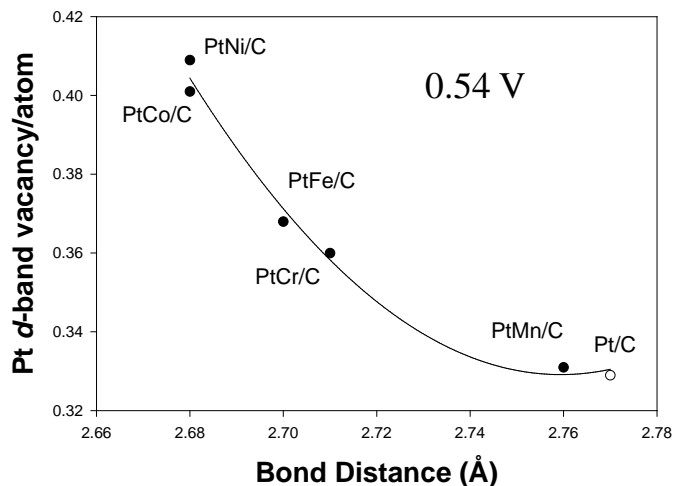
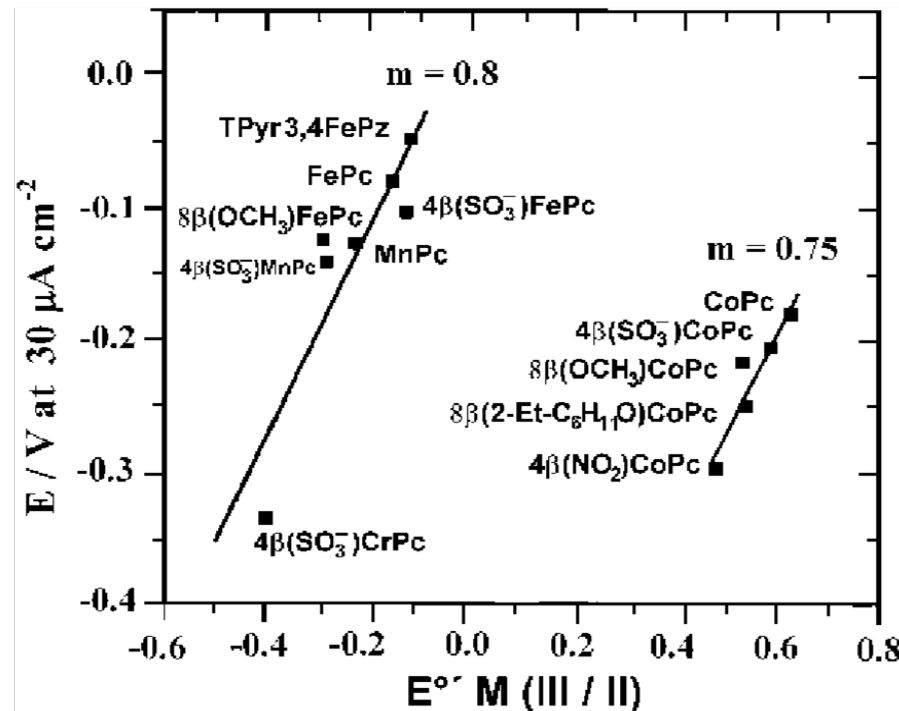
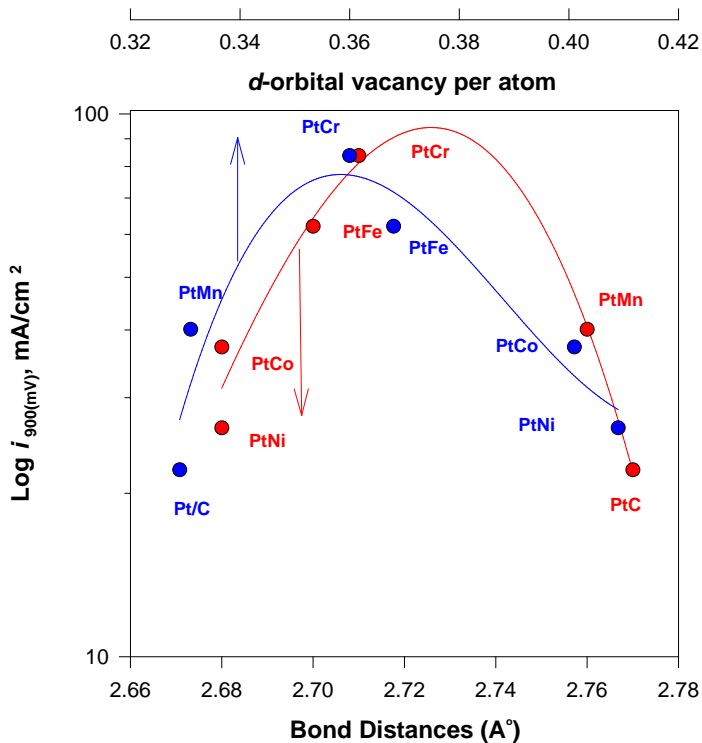


Fe-N₄ sites predominantly yield peroxide in acidic media

Do Volcano Curves Apply?



Pt and Pt Alloys



Evolution studies of ORR active sites as function of pyrolysis temperature in FeTPP structures suggest:

- Direct correlation of Fe²⁺/Fe³⁺ redox potential shift (of FeN₄ center) with temperature, and ORR onset
- In-situ XAS suggest incorporation of Fe-N₄ moieties into graphene layer (upon high temperature treatment) are the active sites
- Presence of other Fe-moieties (Fe-metallic/Fe_xO_y) – unstable in acid/no impact on catalytic activity

LANL PANIFeCo catalyst – at least two stable Fe-moieties present – FeN₄/FeN₂₊₂ and Fe-metallic/Fe_xO_y – both seem to play a role in ORR activity (dual 2x2e mechanism??) – changes of the FT peaks (Fe-Fe, Fe-N/O) together with $\Delta\mu$ signals supports the oxidation of metallic form of Fe and the redox behaviors.

Possibility: *passivation/oxidation of the secondary active site (Fe/Fe_xO_y) at high potentials.*
(Fe-structures similar to most analyzed MNC catalysts with similar ORR performance)

LANL PANI+CN-Fe – same as above, presence of FeN_x and Fe-metallic species observed, with much higher input of the last versus other catalysts at high potentials – no energy shift and no FT peak changes in-situ XAS suggests:

- Possibility1: no passivation of the metallic Fe form through oxidation
- Possibility2: FeN₂₊₂ structure when Fe center is mainly in 3⁺ form from the start
- Possibility3: ‘bridge’ Fe-Fe structure – direct 4e mechanism possible